

**Goldstone-type fluctuations and their implications for the amorphous solid state**Paul M. Goldbart,<sup>1,2</sup> Swagatam Mukhopadhyay,<sup>1</sup> and Annette Zippelius<sup>2,3</sup><sup>1</sup>*Department of Physics, University of Illinois at Urbana-Champaign, Urbana, Illinois 61801-3080, USA*<sup>2</sup>*Kavli Institute for Theoretical Physics, University of California–Santa Barbara, California 93106, USA*<sup>3</sup>*Institut für Theoretische Physik, Universität Göttingen, D-37073 Göttingen, Germany*

(Received 21 March 2004; published 3 November 2004)

In sufficiently high spatial dimensions, the formation of the amorphous (i.e., random) solid state of matter, e.g., upon sufficient crosslinking of a macromolecular fluid, involves particle localization and, concomitantly, the spontaneous breakdown of the (global, continuous) symmetry of translations. Correspondingly, the state supports Goldstone-type low energy, long wavelength fluctuations, the structure and implications of which are identified and explored from the perspective of an appropriate replica field theory. In terms of this replica perspective, the lost symmetry is that of relative translations of the replicas; common translations remain as intact symmetries, reflecting the statistical homogeneity of the amorphous solid state. What emerges is a picture of the Goldstone-type fluctuations of the amorphous solid state as shear deformations of an elastic medium, along with a derivation of the shear modulus and the elastic free energy of the state. The consequences of these fluctuations—which dominate deep inside the amorphous solid state—for the order parameter of the amorphous solid state are ascertained and interpreted in terms of their impact on the statistical distribution of localization lengths, a central diagnostic of the state. The correlations of these order parameter fluctuations are also determined, and are shown to contain information concerning further diagnostics of the amorphous solid state, such as spatial correlations in the statistics of the localization characteristics. Special attention is paid to the properties of the amorphous solid state in two spatial dimensions, for which it is shown that Goldstone-type fluctuations destroy particle localization, the order parameter is driven to zero, and power-law order-parameter correlations hold.

DOI: 10.1103/PhysRevB.70.184201

PACS number(s): 61.43.–j, 82.70.Gg, 64.60.Ak

**I. INTRODUCTION**

The aim of this paper is to identify the long wavelength, low energy fluctuations of the amorphous (i.e., random) solid state, and to investigate their physical consequences. In particular, by constructing an effective free energy that governs these *Goldstone-type* fluctuations, we shall determine the elastic properties of the amorphous solid, including its static shear modulus. We shall also analyze the effect of these fluctuations on the amorphous solid order parameter, and hence determine their impact on physical quantities such as the distribution of localization lengths and the order parameter correlations. Along the way we shall reveal the physical information encoded in these correlations. The treatment presented here is valid deep inside the amorphous solid state, i.e., far from the critical point associated with the phase transition from the liquid to this state. Fluctuation phenomena such as those discussed in the present paper cannot be captured by a solely percolative approach to amorphous solidification. A brief account of the work reported in the present paper has been given elsewhere.<sup>1</sup>

We shall pay particular attention to systems of spatial dimension two, for which we shall see that the effect of fluctuations is strong: particle localization is destroyed, the order parameter is driven to zero, and order-parameter correlations decay as a power law in the separation between points in the sample. Thus we shall see that the amorphous solid state is, in many respects, similar to other states of matter exhibiting (or nearly exhibiting) spontaneously broken continuous symmetry.

This paper is organized as follows. In Sec. II we sketch the properties of the amorphous solid order parameter, in-

cluding the form it takes in the amorphous solid state, focusing on symmetry properties and how they manifest themselves within the replica formalism. In Sec. III we describe the structure of the low energy, long wavelength Goldstone-type excitations of the amorphous solid state in terms of distortions of the value of the order parameter. Here, we also make the identification of these order-parameter distortions as local displacements of the amorphous solid. In Secs. IV and V we determine the energetics of these Goldstone-type excitations by beginning with a Landau-type free energy expressed in terms of the amorphous solid order parameter and ending with elasticity theory. Along the way, we derive a formula for the elastic shear modulus, which shows how this modulus vanishes, as the liquid state is approached, at the classical (i.e., mean-field theory) level. In Sec. VI we discuss the impact of Goldstone-type fluctuations on the structure of the amorphous solid state by examining how they diminish the order parameter and modify the distribution of localization lengths. We analyze the impact of such fluctuations on the order-parameter correlations, and also catalog the various length scales that feature in the paper. In Sec. VII we take a closer look at the effects of Goldstone-type fluctuations on structure and correlations in two-dimensional amorphous solids. In particular, we show that Goldstone-type fluctuations destroy particle localization, the order parameter is driven to zero, and power-law order-parameter correlations hold, and we illustrate these features for certain special cases. In Sec. VIII we discuss the physical content of order-parameter correlations in terms of spatial correlations in the statistics of the localization lengths. We also introduce distributions of correlators, and relate their moments to order-

parameter correlators. Some concluding remarks are given in Sec. IX. Technical details are relegated to four appendixes.

## II. AMORPHOUS SOLID ORDER PARAMETER, SYMMETRIES AND SYMMETRY BREAKING

### A. Order parameter

The solid state of randomly and permanently constrained matter, well exemplified by the rubbery state of vulcanized macromolecular matter, may be detected and characterized via the following order parameter, which depends on an arbitrary number  $\nu (\geq 2)$  of tunable (but nonzero) wave vectors  $\{\mathbf{k}^1, \mathbf{k}^2, \dots, \mathbf{k}^\nu\}$ ,

$$\widetilde{\Omega}(\mathbf{k}^1, \dots, \mathbf{k}^\nu) = \left[ \frac{1}{J} \sum_{j=1}^J \langle e^{i\mathbf{k}^1 \cdot \mathbf{R}_j} \rangle \langle e^{i\mathbf{k}^2 \cdot \mathbf{R}_j} \rangle \dots \langle e^{i\mathbf{k}^\nu \cdot \mathbf{R}_j} \rangle \right]. \quad (1)$$

Here, the vectors  $\{\mathbf{R}_j\}_{j=1}^J$  give the positions of the  $J$  particles that constitute the system; they inhabit a large,  $D$ -dimensional, hypercubic region  $\mathcal{V}$  of volume  $V$ . Angular brackets  $\langle \dots \rangle$  indicate an equilibrium expectation value taken in the presence of a given realization of the quenched random constraints, possibly in a state with spontaneously broken symmetry. Square brackets  $[\dots]$  denote an average over the number and specifications of the quenched random constraints. Periodic boundary conditions discretize the wave vectors  $\mathbf{k}$  to the values  $2\pi\mathbf{m}/V^{1/D}$  in terms of  $D$ -tuples of integers  $\mathbf{m}$ . Additional discussion of this circle of ideas is given in Refs. 2 and 3.

The order parameter (1) detects and diagnoses the amorphous solid state by sensing and quantifying the presence of static random waves in the particle density, as implied by  $\langle e^{i\mathbf{k} \cdot \mathbf{R}_j} \rangle \neq 0$  (for  $\mathbf{k} \neq \mathbf{0}$ ). To acquire some feeling for how it works, consider the illustrative example in which a fraction  $1-Q$  of the particles are unlocalized while the remaining fraction  $Q$  are localized, harmonically and isotropically but randomly, having random mean positions  $\langle \mathbf{R}_j \rangle$  and random mean-square displacements from those positions

$$\langle (\mathbf{R}_j - \langle \mathbf{R}_j \rangle)_d (\mathbf{R}_j - \langle \mathbf{R}_j \rangle)_{d'} \rangle = \delta_{dd'} \xi_j^2, \quad (2)$$

where  $d$  and  $d'$  are Cartesian indices running from 1 to  $D$ . It is straightforward to see that for this example the order parameter becomes

$$\widetilde{\Omega}(\mathbf{k}^1, \dots, \mathbf{k}^\nu) = Q \delta_{\mathbf{0}, \sum_{a=1}^\nu \mathbf{k}^a} \int_0^\infty d\xi^2 \mathcal{N}(\xi^2) \exp\left(-\frac{\xi^2}{2} \sum_{a=1}^\nu |\mathbf{k}^a|^2\right),$$

where

$$\mathcal{N}(\xi^2) \equiv \left[ (QJ)^{-1} \sum_{j \text{ loc}} \delta(\xi^2 - \xi_j^2) \right] \quad (3)$$

is the disorder-averaged distribution of squared localization lengths  $\xi^2$  of the localized fraction of particles.<sup>2-4</sup>

The illustrative example correctly captures the pattern in which symmetry is spontaneously broken when there are enough random constraints to produce the amorphous solid state: microscopically, random localization fully eliminates

translational symmetry; but macroscopically this elimination is not evident. Owing to the absence of any residual symmetry, such as the discrete translational symmetry of crystallinity, all macroscopic observables are those of a translationally invariant system. This shows up as the vanishing of the order parameter, even in the amorphous solid state, unless the wave vectors sum to zero, i.e.,  $\sum_{a=1}^\nu \mathbf{k}^a = \mathbf{0}$ .

The case  $\nu=1$  is excluded from the list of order parameter components shown in Eq. (1). This case corresponds to *macroscopic* density fluctuations, and these are assumed to remain small and stable (i.e., noncritical) near the amorphous solidification transition, being suppressed by forces, such as the excluded-volume interaction, that tend to maintain homogeneity. Additional insight into the nature of the constraint-induced instability of the liquid state and its resolution (in terms of the formation of the amorphous solid state—a mechanism for evading macroscopic density fluctuations) is given in Ref. 3, especially Sec. 4.2.

### B. Symmetries and symmetry breaking; replica formulation

How does the order parameter (1) transform under translations of the particles? If, in the element  $\langle \exp i\mathbf{k}^a \cdot \mathbf{R}_j \rangle$ , one makes the translation  $\mathbf{R}_j \rightarrow \mathbf{R}_j + \mathbf{r}^a$  then the element is multiplied by a factor  $\exp i\mathbf{k}^a \cdot \mathbf{r}^a$  and so the order parameter acquires a factor  $\exp i\sum_{a=1}^\nu \mathbf{k}^a \cdot \mathbf{r}^a$ . Now, in the fluid state no particles are localized and the order parameter has the value zero, so it is invariant under the aforementioned translations. By contrast, in the amorphous solid state the order parameter is nonzero, provided the wave vectors sum to zero. Thus, the order parameter varies under the translations unless the translation is common to each element, i.e.,  $\mathbf{r}^a = \mathbf{r}$ . To summarize, the liquid-state symmetry of the independent translations of the elements is broken down, at the amorphous solidification transition, to the residual symmetry of the common translation of the elements.

When replicas are employed to perform the average over the quenched disorder (i.e., the number and location of the constraints), what emerges is a theory of a field  $\hat{\Omega}(x)$  defined over  $(1+n)$ -fold replicated space  $x$ , so that the argument  $x$  means the collection of  $(1+n)$  position  $D$ -vectors  $\{\mathbf{x}^0, \mathbf{x}^1, \dots, \mathbf{x}^n\}$  conjugate to the wave vectors  $\{\mathbf{k}^0, \mathbf{k}^1, \dots, \mathbf{k}^n\}$ . It is understood that the limit  $n \rightarrow 0$  is to be taken at the end of any calculation. In terms of replicas, the expectation value of this field  $\langle \hat{\Omega}(x) \rangle$  is proportional to

$$\left\langle \prod_{j=1}^J \sum_{\alpha=0}^n \delta(\mathbf{x}^\alpha - \mathbf{R}_j^\alpha) \right\rangle \quad (4)$$

and its Fourier transform  $\Omega(k) = \int dx \exp(ik \cdot x) \hat{\Omega}(x)$ , has the form

$$\Omega(k) = \left\langle \prod_{j=1}^J \sum_{\alpha=0}^n \exp i \sum_{\alpha=0}^n \mathbf{k}^\alpha \cdot \mathbf{R}_j^\alpha \right\rangle. \quad (5)$$

The field  $\hat{\Omega}(x)$  fluctuates subject to the demand, mentioned above, that the critical freedoms are only the corresponding Fourier amplitudes  $\Omega(k)$  for which at least two of the

$D$ -component entries in the argument  $k \equiv \{\mathbf{k}^0, \mathbf{k}^1, \dots, \mathbf{k}^n\}$  are nonzero. Both a semimicroscopic approach and arguments based on symmetries and length scales yield a Landau-Wilson effective Hamiltonian governing the fluctuations of this field, which is invariant under independent translations of the replicas but whose precise structure we shall discuss later. For now, let us just mention that the corresponding expectation value of this field is the order parameter (1) with  $\nu=1+n$ : it becomes nonzero in the amorphous solid state and, in doing so, realizes the pattern of spontaneous symmetry breaking described above. Invariance under independent translations of the replicas breaks down to invariance under the subgroup of common translations of the replicas.

### III. GOLDSTONE FLUCTUATIONS: STRUCTURE AND IDENTIFICATION

#### A. Formal construction of Goldstone fluctuations

In the amorphous solid state, one of the symmetry-related family of classical values of the order parameter has the form

$$\Omega(k) = \delta_{\mathbf{k}_{\text{tot}}, 0} \mathcal{W}(k_\tau) = \int_V \frac{d\mathbf{x}_{\text{c.m.}}}{V} e^{i\mathbf{k}_{\text{tot}} \cdot \mathbf{x}_{\text{c.m.}}} \mathcal{W}(k_\tau), \quad (6)$$

in which  $\mathcal{W}$  is real and depends only on the magnitude of  $k_\tau$ . Some geometry is needed to define the variables in this formula. We introduce a complete orthonormal basis set in replica space  $\{\epsilon^\alpha\}_{\alpha=0}^n$ , in terms of which vectors  $k$  are expressed as

$$k = \sum_{\alpha=0}^n \mathbf{k}^\alpha \epsilon^\alpha. \quad (7)$$

We also introduce the *replica body-diagonal* unit vector

$$\epsilon \equiv \frac{1}{\sqrt{1+n}} \sum_{\alpha=0}^n \epsilon^\alpha, \quad (8)$$

relative to which we may decompose vectors  $k$  into longitudinal ( $\lambda$ ) and transverse ( $\tau$ ) components,

$$k = k_\lambda + k_\tau, \quad k_\lambda \equiv (k \cdot \epsilon)\epsilon, \quad k_\tau \equiv k - (k \cdot \epsilon)\epsilon. \quad (9)$$

We find it convenient to parametrize the longitudinal components of position and wave vectors in the following distinct ways:

$$x_\lambda = (1+n)^{1/2} \mathbf{x}_{\text{c.m.}} \cdot \epsilon, \quad \mathbf{x}_{\text{c.m.}} \equiv \frac{1}{1+n} \sum_{\alpha=0}^n \mathbf{x}^\alpha, \quad (10a)$$

$$k_\lambda = (1+n)^{-1/2} \mathbf{k}_{\text{tot}} \cdot \epsilon, \quad \mathbf{k}_{\text{tot}} \equiv \sum_{\alpha=0}^n \mathbf{k}^\alpha. \quad (10b)$$

Then  $\mathbf{x}_{\text{c.m.}}$  and  $\mathbf{k}_{\text{tot}}$  are, respectively, the analogs of the following conjugate pair of vectors: the center-of-mass position and the total momentum. With them one then has, e.g.,  $k_\lambda \cdot x_\lambda = \mathbf{k}_{\text{tot}} \cdot \mathbf{x}_{\text{c.m.}}$ .

The variables just introduced exhibit the structure of a classical state Eq. (6) as a rectilinear *hill* in  $x$  space, with

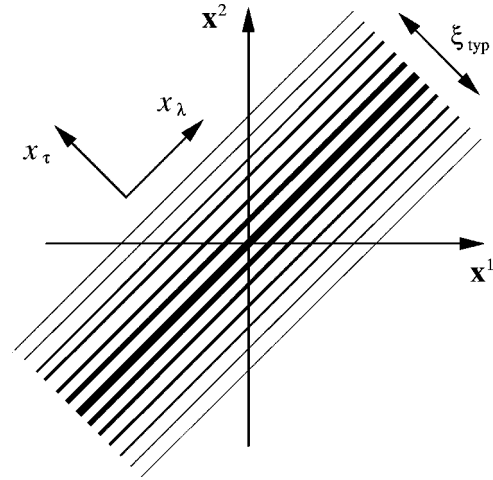


FIG. 1. A classical state in replicated real space: a hill in  $x$  space with its ridge aligned in the  $x_\lambda$  direction and passing through the origin. The thickness of the lines is intended to suggest the amplitude of the order parameter, the thicker the line the larger the amplitude. Symmetry-related classical states follow from rigid displacements of the hill perpendicular to the ridge, i.e., in the  $x_\tau$  direction.

contours of constant height oriented along  $x_\lambda$ , as shown in Fig. 1. The peak height of the ridge determines the fraction of localized particles; the decay of the height in the direction  $x_\tau$  determines the distribution of localization lengths. The width of the hill corresponds to the typical value of the localization length. Symmetry-related classical states are generated from Eq. (6) by translating the hill rigidly, perpendicular to the ridge line (i.e., parallel to  $x_\tau$ ). Such a transformation corresponds to relative (but not common) translations of the replicas. (See Fig. 2.)

This pattern of symmetry breaking suggests that the Goldstone excitations of a classical state are constructed from it

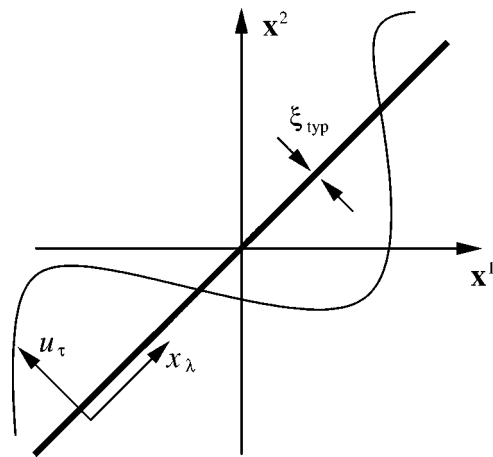


FIG. 2. Goldstone-distorted state in replicated real space: the hill is displaced perpendicular to the ridge to an extent  $u_\tau$  that varies with position  $x_\lambda$  along the ridge. Note that the scale of this figure is much larger than that used for Fig. 1: the thick line lies along the ridge of the classical state, but now it is the *width* of the line that indicates the width of the hill  $\xi_{\text{typ}}$ . The Goldstone-type fluctuations occur on wavelengths longer than  $\xi_{\text{typ}}$ .

via  $x_\lambda$  (or equivalently  $\mathbf{x}_{c.m.}$ )-dependent translations of the hill in the  $x_\tau$  direction, i.e., ripples of the hill and its ridge. In two equivalent realizations, this gives

$$V\Omega(k) = \int_{\mathcal{V}} d\mathbf{x}_{c.m.} e^{i\mathbf{k}_{tot}\cdot\mathbf{x}_{c.m.}+ik_\tau u_\tau(\mathbf{x}_{c.m.})} \mathcal{W}(k_\tau), \quad (11a)$$

$$V\hat{\Omega}(x) = \hat{\mathcal{W}}[x_\tau - u_\tau(\mathbf{x}_{c.m.})]. \quad (11b)$$

Note that we are choosing to define Fourier transforms as follows:

$$\hat{A}(x) = \int dk_\tau d\mathbf{k}_{tot} e^{-ik_\tau x_\tau} e^{-i\mathbf{k}_{tot}\cdot\mathbf{x}_{c.m.}} A(k), \quad (12a)$$

$$A(k) = \int dx_\tau d\mathbf{x}_{c.m.} e^{ik_\tau x_\tau} e^{i\mathbf{k}_{tot}\cdot\mathbf{x}_{c.m.}} \hat{A}(x); \quad (12b)$$

also note that

$$\hat{\mathcal{W}}(x_\tau) \equiv \int dk_\tau e^{-ik_\tau x_\tau} \mathcal{W}(k_\tau). \quad (12c)$$

Here and elsewhere, bars indicate division by factors of  $2\pi$ ; on integration measures there is one such division for each variable of integration. The details of the excitation are encoded in the replica-transverse field  $u_\tau(\mathbf{x}_{c.m.})$ , an  $nD$ -component field that depends on the replica-longitudinal position  $\mathbf{x}_{c.m.}$ ; these are the *Goldstone bosons*, or phonon excitations, of the amorphous solid state. For consistency, we require that the Fourier content of the Goldstone field  $u_\tau(\mathbf{x}_{c.m.})$  occurs at wavelengths long compared with the hill width (i.e., the typical localization length). Otherwise the energy of the field  $u_\tau(\mathbf{x}_{c.m.})$  would be comparable to other excitations which have been neglected.

The Goldstone excitations that we have just constructed are analogs of the capillary excitations of the interface between coexisting liquid and gas states; see Ref. 5 for a review. In the liquid-gas context they similarly accompany a spontaneous breaking of translational symmetry associated with the choice of interface location.

Do the Goldstone excitations exhaust the spectrum of low energy excitations of the broken-symmetry state? The complete spectrum of excitations is accounted for by decorating the Goldstone-type parametrization (11a) with additional freedoms  $w(k_\tau)$ , so that the field  $\Omega(k)$  is expressed as

$$V\Omega(k) = \int_{\mathcal{V}} d\mathbf{x}_{c.m.} e^{i\mathbf{k}_{tot}\cdot\mathbf{x}_{c.m.}+ik_\tau u_\tau(\mathbf{x}_{c.m.})} (\mathcal{W}(k_\tau) + w(k)), \quad (13)$$

where  $w$  is a real-valued field that depends on  $k_\tau$ , suitably constrained to be independent of the Goldstone excitations. To see that the Goldstone modes (11a) do indeed exhaust the spectrum of low energy excitations, we make contact with the linear stability analysis of the classical broken-symmetry state, due to Castillo *et al.*,<sup>6</sup> which identified a family of linearly additive Goldstone-type normal modes of excitation indexed by  $\mathbf{k}_{tot}$ ,

$$V\Omega(k) = \int_{\mathcal{V}} d\mathbf{x}_{c.m.} e^{i\mathbf{k}_{tot}\cdot\mathbf{x}_{c.m.}} \mathcal{W}(k_\tau) + ik_\tau \cdot v_\tau(\mathbf{k}_{tot}) \mathcal{W}(k_\tau), \quad (14)$$

with arbitrary replica-transverse amplitude  $v_\tau(\mathbf{k}_{tot})$ . That this linear glimpse of the Goldstone-type excitations is in accordance with the nonlinear view focused on in the present paper follows by expanding Eq. (13) to linear order in the Goldstone fields  $u_\tau$  and omitting the non-Goldstone fields  $w$ , thus arriving at

$$V\Omega(k) \approx \int_{\mathcal{V}} d\mathbf{x}_{c.m.} e^{i\mathbf{k}_{tot}\cdot\mathbf{x}_{c.m.}} \mathcal{W}(k_\tau) + ik_\tau \cdot \int_{\mathcal{V}} d\mathbf{x}_{c.m.} e^{i\mathbf{k}_{tot}\cdot\mathbf{x}_{c.m.}} u_\tau(\mathbf{x}_{c.m.}) \mathcal{W}(k_\tau), \quad (15)$$

which shows that  $v_\tau(\mathbf{k}_{tot})$  is the Fourier transform of  $u_\tau(\mathbf{x}_{c.m.})$ . The reality of  $\Omega(x)$  ensures that  $\Omega(-k) = \Omega(k)^*$  and, via Eq. (14), that  $v_\tau(-\mathbf{k}_{tot}) = v_\tau(\mathbf{k}_{tot})^*$ . Via Eq. (15), this in turn ensures the reality of  $u_\tau(\mathbf{x}_{c.m.})$ . In Ref. 6 it was shown that no other branches of low energy excitations exist; hence the Goldstone excitations of Eq. (11a) exhaust the spectrum of low energy excitations.

Some insight into the structure of the Goldstone excitations, which induce deformations of the classical state, is obtained from its replicated real-space version. Consider the interpretation of  $\hat{\Omega}(x)$  as a quantity proportional to the probability density for the positions of the  $1+n$  replicas of a particle to have the values  $\{\mathbf{x}^\alpha\}_{\alpha=0}^n$ ; see Eq. (4). Then classical states, Eq. (11b) at constant  $u_\tau$ , are ones that describe a translationally invariant *bound states*:  $\hat{\Omega}(x)$  does not depend on the *mean* location of the replicas  $\mathbf{x}_{c.m.}$ , but does depend on their *relative* locations, through  $x_\tau$  and decays the more the replicas are separated. This point is exemplified by the particular form given in Eq. (26a). Now, the Goldstone-distorted state, Eq. (11b) with  $u_\tau$  varying with  $\mathbf{x}_{c.m.}$ , also describes bound states of the replicas, but ones in which the dependence of the probability density on relative locations varies with  $\mathbf{x}_{c.m.}$ . The particular form (26a), which gives

$$V\hat{\Omega}(x) = \mathcal{Q} \int_0^\infty d\xi^2 \mathcal{N}(\xi^2) (2\pi\xi^2)^{-nD/2} \times \exp(-|x_\tau - u_\tau(\mathbf{x}_{c.m.})|^2/2\xi^2), \quad (16)$$

exemplifies this point; in particular, one sees that the most probable value  $u_\tau$  of the *relative* locations  $x_\tau$  now depends on the *center-of-mass* location  $\mathbf{x}_{c.m.}$ . These remarks are amplified in Fig. 3.

Returning to the issue of the structure and properties of the Goldstone-type excitations of the amorphous solid state, recall that the critical Fourier amplitudes of the field are those that reside in the higher-replica sector [i.e., HRS, for which at least two  $D$ -vector elements of the argument of  $\Omega(k)$  are nonzero]. Do the proposed Goldstone distortions of

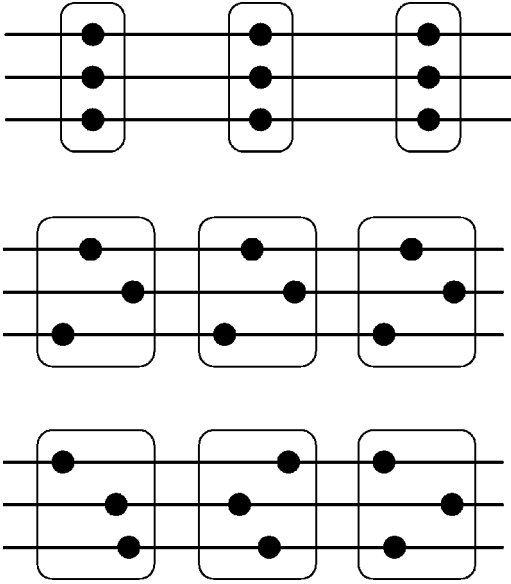


FIG. 3. *Molecular bound state view of the classical and Goldstone-distorted states in replicated real space.* The full circles within a border represent the replicas of a given monomer location. Repetitions of them along a row indicate that the center of mass of the bound state is distributed homogeneously. Upper bars, one classical state; the probability density is peaked at the shown configurations, in a manner independent of the location of the center of mass of the bound state of the replicated particles. Middle bars, another classical state, obtained by the former one via a relative translation of the replicas that does not vary with the location of the center of mass. Lower bars, a Goldstone-distorted state; the probability density is peaked in a manner that varies with the location of the center of mass.

the classical state excite the lower-replica sectors; If so, they would be suppressed by interactions, such as particle repulsion, that tend to preserve homogeneity. To see that they do not, let us examine the Goldstone-distorted state in the zero- (i.e.,  $k=0$ ) and one- (i.e.,  $k=\mathbf{q}\epsilon^\alpha$  with  $\mathbf{q} \neq \mathbf{0}$ ) replica sectors. In the former, one readily sees from Eq. (11a) that it has its undistorted value. A straightforward calculation shows that in the latter sector the distorted order parameter contains the factor

$$\int_V \frac{d\mathbf{x}_{c.m.}}{V} \exp(i\mathbf{q} \cdot \mathbf{x}_{c.m.} + i\mathbf{q} \cdot \mathbf{u}^\alpha(\mathbf{x}_{c.m.})), \quad (17)$$

where  $\mathbf{u}^\alpha = u_\tau \cdot \epsilon^\alpha$ . By introducing the transformation  $\mathbf{x}_{c.m.} \rightarrow \mathbf{x}'_{c.m.} \equiv \mathbf{x}_{c.m.} + \mathbf{u}^\alpha(\mathbf{x}_{c.m.})$  we see that the Goldstone-distorted state remains zero in the one-replica sector, provided all  $D$ -vector elements  $\mathbf{u}^\alpha$  of the Goldstone field  $u_\tau(\mathbf{x}_{c.m.})$  obey the condition

$$|\det(\delta_{dd'} + \partial_d u_{d'}^\alpha)| = 1, \quad (18)$$

which, for small amplitude distortions, reduces to  $\partial_d u_{d'}^\alpha = 0$ . That this condition corresponds to incompressibility (i.e., *pure shear*) will be established in Sec. III B. (Here and elsewhere, summations from 1 to  $D$  are implied over repeated Cartesian indices, such as  $d$  and  $d'$ .) This is as it should be,

to make density fluctuations there must be some compression amongst the elements  $\mathbf{u}^\alpha$  of  $u_\tau$ .

### B. Identifying the Goldstone fluctuations as local displacements

In this section our aim is to establish the connection between the Goldstone fields and the displacement fields of conventional elasticity theory,<sup>7,8</sup> *Inter alia*, this identifies the stiffness associated with the Goldstone fluctuations as the elastic modulus governing shear deformations of the amorphous solid. As we shall see, the discussion is general enough to apply to *any* amorphous solid that breaks translational symmetry microscopically but preserves it macroscopically, in regimes where the constituent particles are strongly localized in position.

Recall the amorphous solid order parameter, Eq. (1),

$$\left[ \mathcal{J}^{-1} \sum_{j=1}^J \langle e^{i\mathbf{k}^1 \cdot \mathbf{R}_j} \rangle \langle e^{i\mathbf{k}^2 \cdot \mathbf{R}_j} \rangle \dots \langle e^{i\mathbf{k}^v \cdot \mathbf{R}_j} \rangle \right],$$

and focus on a single element  $\langle e^{i\mathbf{k} \cdot \mathbf{R}_j} \rangle$ . It is convenient to consider the element in the form

$$e^{i\mathbf{k} \cdot \mathbf{r}_j / \rho_j(\mathbf{k})}, \quad (19)$$

where  $\mathbf{r}_j$  is the mean of the position of particle  $j$ , and  $\rho_j$  describes fluctuations about the mean. Now consider the impact of a long wavelength shear displacement, encoded in the field  $\mathbf{v}(\mathbf{x})$ , which deforms the probability density associated with the position  $\mathbf{R}_j$  of particle  $j$ . By assuming that the typical localization length is much smaller than the length scale associated with variations of the deformation we are able to retain only the *rigid* displacement of the probability density for  $\mathbf{R}_j$  and neglect any deformation of its *shape*. Thus, under the displacement the element is deformed as

$$\langle e^{i\mathbf{k} \cdot \mathbf{R}_j} \rangle = e^{i\mathbf{k} \cdot \mathbf{r}_j / \rho_j(\mathbf{k})} \rightarrow e^{i\mathbf{k} \cdot (\mathbf{r}_j + \mathbf{v}(\mathbf{r}_j)) / \rho_j(\mathbf{k})}. \quad (20)$$

Inserting such deformations into the order parameter, with an independent displacement field for each element, gives the distorted form

$$\begin{aligned} & \left[ \frac{1}{J} \sum_{j=1}^J e^{i\sum_{a=1}^v \mathbf{k}^a \cdot \mathbf{r}_j} e^{i\sum_{a=1}^v \mathbf{k}^a \cdot \mathbf{v}^a(\mathbf{r}_j)} \rho_j(\mathbf{k}^1) \dots \rho_j(\mathbf{k}^v) \right] \\ & = \int \frac{d\mathbf{r}}{V} e^{i\sum_{a=1}^v \mathbf{k}^a \cdot (\mathbf{r} + \mathbf{v}^a(\mathbf{r}))} [\rho_j(\mathbf{k}^1) \dots \rho_j(\mathbf{k}^v)], \end{aligned} \quad (21)$$

where we have arrived at the second form by noting that, in the amorphous solid state, the mean position of any particle is distributed homogeneously. Next, we decompose the collection of displacement fields  $\{\mathbf{v}^a\}$  into longitudinal and transverse parts, according to the geometrical prescription given in Sec. III A, but keeping in mind the fact that there are now  $v$  copies (rather than  $1+n$ ). The essential point is that the longitudinal part of  $\{\mathbf{v}^a\}$ , which corresponds to *common* deformations of the elements, does not generate a new value of the order parameter, in contrast with the transverse part (which generates *relative* deformations). Therefore, the *physical* displacements are the transverse part of  $\{\mathbf{v}^a\}$ . To see

this point, consider the special situation in which the transverse part of  $\{\mathbf{v}^a\}$  is position dependent but the longitudinal part is *not*. In this case, ( $V$  times) the order parameter becomes

$$\int d\mathbf{r} e^{i\sum_{a=1}^p \mathbf{k}^a \cdot \mathbf{r}} e^{ik_\tau v_\tau(\mathbf{r}) + i\mathbf{k}_{\text{tot}} \cdot \mathbf{v}_{\text{c.m.}}} [\rho_j(\mathbf{k}^1) \cdots \rho_j(\mathbf{k}^p)]. \quad (22)$$

As things stand, in the presence of  $v_\tau(\mathbf{r})$ , a longitudinal part  $\mathbf{v}_{\text{c.m.}}$  would have the effect of producing a new value of the order parameter. As, on physical grounds, we expect that it should not, we see that *physical* displacements are purely transverse. This is a consequence of the fact that, for the long wavelength displacements under consideration, the deformed amorphous solid state continues to preserve translational invariance macroscopically. This argument for the absence of the longitudinal part of the displacement field continues to hold when it has position dependence: if, when constant, it does not generate a new state degenerate with the old one then, when varying, it should not generate a low-energy deformation.

Thus we have realized the goal of this section: by comparing Eqs. (11a) and (22) we see that the formally constructed Goldstone fields  $u_\tau$  are in fact the physical displacement fields  $v_\tau$ . Actually, there is one further point to address, concerning the argument of the final factor in Eq. (22), viz.  $[\rho_j(\mathbf{k}^1) \cdots \rho_j(\mathbf{k}^p)]$ . Apparently, there is dependence on the full set of wave vectors  $\{\mathbf{k}^1, \dots, \mathbf{k}^p\}$ , whereas Eq. (11a) indicates dependence only on the transverse part of this collection. The resolution of this apparent discrepancy lies in the observation that, for position independent  $v_\tau$ , Eq. (22) must revert to a classical state, for which the final factor does not depend on  $\mathbf{k}_{\text{tot}}$ . As the final factor consists of probability clouds, which we are assuming to be undeformed by the displacements, this factor continues to be independent of  $\mathbf{k}_{\text{tot}}$  in Eq. (22).

#### IV. ENERGETICS OF GOLDSTONE FLUCTUATIONS; ELASTIC FREE ENERGY

The simplest Landau-Wilson effective Hamiltonian controlling the order parameter  $\Omega$  has the form

$$\begin{aligned} \mathcal{S}_\Omega = & Vc \sum_{k \in \text{HRS}} \left( -a\tau + \frac{1}{2} \xi_0^2 k \cdot k \right) \Omega(k) \Omega(-k) \\ & - Vcg \sum_{k_1, k_2, k_3 \in \text{HRS}} \delta_{k_1 + k_2 + k_3, 0} \Omega(k_1) \Omega(k_2) \Omega(k_3), \end{aligned} \quad (23)$$

where  $c$  is the number of entities being constrained per unit volume, and  $\{a\tau, \xi_0, g\}$  are, respectively, the control parameter for the density of constraints, the linear size of the underlying objects being linked, and the nonlinear coupling constant controlling the strength with which the  $\Omega$  fluctuations interact. HRS indicates that only wave vectors in the higher-replica sector are to be included in the summations. A semimicroscopic model of vulcanized macromolecular matter yields  $a=1/2$ ,  $\tau=(m^2-m_c^2)/m_c^2$ ,  $\xi_0^2=L\ell_p/2D$ , and  $g=1/6$ , where  $m$  controls the mean number of constraints (and has critical value  $m_c=1$ ),  $\ell_p$  is the persistence length of the mac-

romolecules, and  $L/\ell_p$  is the number of segments per macromolecule.

In terms of  $\mathcal{S}_\Omega$ , the replica partition function  $\mathcal{Z}_{1+n}$  is given integrating over the critical modes of  $\Omega$ ,

$$\mathcal{Z}_{1+n} \sim \int \mathcal{D}\Omega e^{-\mathcal{S}_\Omega}. \quad (24)$$

Then, according to the replica scheme of Deam and Edwards,<sup>9</sup> the disorder-averaged free energy  $F$  is given by

$$-\frac{F}{T} = \lim_{n \rightarrow 0} \frac{\mathcal{Z}_{1+n} - \mathcal{Z}_1}{n\mathcal{Z}_1} = \lim_{n \rightarrow 0} \frac{\partial}{\partial n} \ln \mathcal{Z}_{1+n}, \quad (25)$$

where  $T$  is the temperature.

It was shown in Ref. 4 (see also Refs. 2, 3, and 10) that making  $\mathcal{S}_\Omega$  stationary with respect to  $\Omega$  results in the classical state (6), with

$$\mathcal{W}(k_\tau) = Q \int_0^\infty d\xi^2 \mathcal{N}(\xi^2) e^{-\xi^2 k_\tau^2 / 2}, \quad (26a)$$

$$Q = 2a\tau/3g, \quad (26b)$$

$$\mathcal{N}(\xi^2) = (\xi_0^2/a\tau\xi^4) \pi(\xi_0^2/a\tau\xi^2), \quad (26c)$$

where  $\pi(\theta)$  is the universal classical scaling function discussed in Refs. 4 and 10. Distorting the classical state, via Eq. (11a) or (11b), inserting the resulting state into  $\mathcal{S}_\Omega$  and computing the *increase*,  $\mathcal{S}_u$ , in  $\mathcal{S}_\Omega$  due to the distortion  $u_\tau$  (i.e., the elastic free energy) gives the following contribution, which arises solely from the quadratic ‘‘gradient’’ term in  $\mathcal{S}_\Omega$ :

$$\mathcal{S}_u = \frac{\mu_n}{2T} \int_V d\mathbf{x} (\partial_{\mathbf{x}} u_\tau \cdot \partial_{\mathbf{x}} u_\tau), \quad (27a)$$

$$\mu_n \equiv \frac{Tc}{(1+n)^{1+D/2}} \int V^n dk_\tau \frac{\xi_0^2 k_\tau^2}{nD} \mathcal{W}(k_\tau)^2, \quad (27b)$$

in the former of which there are scalar products over both the  $nD$  independent components of  $u_\tau$  and the  $D$  components of  $\mathbf{x}$ . The derivation of this elastic free energy is given in Appendix A. As we have discussed in Sec. III B, and shall revisit in Sec. V,  $\mu_0$  is the elastic shear modulus. By using the specific classical form for  $\mathcal{W}$ , Eq. (26a), and passing to the replica limit,  $n \rightarrow 0$ , we obtain

$$\mu_0 = TcQ^2 \int d\xi^2 \mathcal{N}(\xi^2) d\xi'^2 \mathcal{N}(\xi'^2) \frac{\xi_0^2}{\xi^2 + \xi'^2} \quad (28a)$$

$$= Tc\tau^3 \frac{4a^2}{9g^2} \int d\theta d\theta' \frac{\pi(\theta)\pi(\theta')}{\theta^{-1} + \theta'^{-1}} \quad (28b)$$

which, for the case of the semimicroscopic parameters stated shortly after Eq. (23), becomes

$$\mu_0 = 2Tc\tau^3 \int d\theta d\theta' \frac{\pi(\theta)\pi(\theta')}{\theta^{-1} + \theta'^{-1}}. \quad (28c)$$

The main technical steps of this derivation are given in Appendix B. Thus, we have arrived at the effective free energy controlling elastic deformations, in the harmonic approximation. It is consistent with the result obtained in Ref. 11, in which the free energy cost of imposing a macroscopic shear deformation of the sample was determined.

### V. IDENTIFICATION OF THE SHEAR MODULUS: MACROSCOPIC VIEW

In Sec. III B, we have explained why the Goldstone-type fluctuations are identified with local displacements of the amorphous solid by considering the impact of these fluctuations at a semimicroscopic level. In the present section we again address this identification, but now from a more macroscopic perspective, by coupling the Goldstone fields to a force-density field.

Accounting solely for the Goldstone-type fluctuations [i.e., ignoring the field  $w$  in the parametrization of the field  $\Omega$  in Eq. (13)], we approximate the replica partition function (24) as

$$\begin{aligned} \mathcal{Z}_{1+n}[f_\tau] &\sim e^{-S_{\Omega,cl}} \int \mathcal{D}u_\tau \exp\left(-\frac{\mu_0}{2T} \int_{\mathcal{V}} d\mathbf{x} \partial_{\mathbf{x}} u_\tau \cdot \partial_{\mathbf{x}} u_\tau \right. \\ &\quad \left. + \frac{1}{T} \int_{\mathcal{V}} d\mathbf{x} f_\tau(\mathbf{x}) \cdot u_\tau(\mathbf{x})\right), \end{aligned} \quad (29)$$

in which  $S_{\Omega,cl}$  is the effective free energy (23) evaluated in the classical state (6), and  $\mathcal{D}u_\tau$  indicates functional integration over replicated displacement fields  $\{\mathbf{u}^\alpha(\mathbf{x})\}$  subject to the following conditions:  $u$  is replica-transverse [cf. Eq. (9)]; the  $D$ -vector elements it contains are pure shear [cf. Eq. (18)]; and the Fourier content is restricted to wavelengths longer than a short-distance cutoff  $\ell_<$  (which is we take to be on the order of the typical localization length) but shorter than a long-distance cutoff  $\ell_>$  (which is commonly on the order of the linear size of the sample). The reason for the restriction to wavelengths longer than the typical localization length is that by restricting our attention to the Goldstone sector of fluctuations we are omitting the effects of massive fluctuations. To be consistent, we should also omit the effects of Goldstone-type fluctuations with wavelengths sufficiently short that their energy scale is comparable to or larger than the scale for the (omitted) least massive fluctuations. The appropriate criterion is that the short-distance cutoff be taken to be on the order of the typical localization length. This can be appreciated pictorially from Figs. 1 and 2: Goldstone-type fluctuations having wavelengths smaller than the hill width are omitted. Note that we have ignored the Jacobian factor connected with the change of functional integration variable from  $\Omega$  to  $u$ .

In order to reconfirm the identification of the shear modulus, we have, in Eq. (29), coupled the displacement field  $u$  linearly to a replicated *force density field*  $f$  though a term

$-1/T \int d\mathbf{x} f(\mathbf{x}) \cdot u(\mathbf{x})$ ; because  $u_\lambda$  is zero, only the transverse term,  $-1/T \int d\mathbf{x} f_\tau(\mathbf{x}) \cdot u_\tau(\mathbf{x})$ , remains. As for  $f$  itself, it is taken to have  $D$ -vector elements that vanish in the zeroth replica and are identically equal to  $\mathbf{f}$  in the remaining replicas. This reflects the fact that the force density is envisaged as being applied *subsequent* to the cross-linking process, and therefore does not feature in the replica that generates the cross-link distribution, but is repeated in the *thermodynamic* replicas (by which we mean the replicas that generate the logarithm of the partition function, not the disorder distribution). Thus, one has

$$f_\tau \cdot f_\tau = f \cdot f - f_\lambda \cdot f_\lambda = n\mathbf{f} \cdot \mathbf{f} - (f \cdot \boldsymbol{\epsilon})^2 = \frac{n}{1+n} \mathbf{f} \cdot \mathbf{f} \xrightarrow{n \rightarrow 0} n\mathbf{f} \cdot \mathbf{f}. \quad (30)$$

The integration over  $u$  in Eq. (29) is Gaussian, and thus straightforward, requiring only the elastic correlator  $\langle u_d(\mathbf{y})u_{d'}(\mathbf{y}') \rangle$ , which is given in terms of the elastic Green function  $\mathcal{G}_{dd'}(\mathbf{y}-\mathbf{y}')$ ,

$$\begin{aligned} \langle u_d(\mathbf{y})u_{d'}(\mathbf{y}') \rangle &= \frac{\int \mathcal{D}\mathbf{u} \exp\left(-\frac{\mu_0}{2T} \int_{\mathcal{V}} d\mathbf{x} \partial_{\mathbf{x}} \mathbf{u} \cdot \partial_{\mathbf{x}} \mathbf{u}\right) u_d(\mathbf{y})u_{d'}(\mathbf{y}')}{\int \mathcal{D}\mathbf{u} \exp\left(-\frac{\mu_0}{2T} \int_{\mathcal{V}} d\mathbf{x} \partial_{\mathbf{x}} \mathbf{u} \cdot \partial_{\mathbf{x}} \mathbf{u}\right)} \\ &= \frac{T}{\mu_0} \mathcal{G}_{dd'}(\mathbf{y}-\mathbf{y}'), \end{aligned} \quad (31a)$$

$$\begin{aligned} \mathcal{G}_{dd'}(\mathbf{y}) &= \int_{2\pi/\ell_>}^{2\pi/\ell_<} d\mathbf{k} e^{-i\mathbf{k}\cdot\mathbf{y}} \mathcal{G}_{dd'}(\mathbf{k}), \\ \mathcal{G}_{dd'}(\mathbf{k}) &= (k^2 \delta_{dd'} - k_d k_{d'}) / k^4, \end{aligned} \quad (31b)$$

where  $\ell_>$  and  $\ell_<$  are, respectively, the long- and short-distance cutoffs on the wave-vector integration, mentioned above. This elastic Green function will be derived in Appendix C. In terms of the elastic Green function and the force density, one finds for the increase  $F[\mathbf{f}] - F[0]$  in free energy due to the applied force-density field,

$$\begin{aligned} F[\mathbf{f}] - F[0] &= -T \lim_{n \rightarrow 0} \frac{\mathcal{Z}_{1+n}[\mathbf{f}] - \mathcal{Z}_{1+n}[0]}{n\mathcal{Z}_1[0]} \\ &= -T \lim_{n \rightarrow 0} \frac{\partial}{\partial n} \ln \frac{\mathcal{Z}_{1+n}[\mathbf{f}]}{\mathcal{Z}_{1+n}[0]} \end{aligned} \quad (32a)$$

$$\approx -\frac{1}{2\mu_0} \int_{\mathcal{V}} d\mathbf{x} d\mathbf{x}' \sum_{d,d'=1}^D f_d(\mathbf{x}) \mathcal{G}_{dd'}(\mathbf{x}-\mathbf{x}') f_{d'}(\mathbf{x}'), \quad (32b)$$

which indicates that  $\mu_0$  is the shear modulus; see Refs. 7 and 8.

## VI. EFFECT OF GOLDSTONE FLUCTUATIONS ON THE ORDER PARAMETER AND ITS CORRELATIONS

In this section we discuss, how Goldstone fluctuations affect the expectation value and the correlations of the order parameter. Our discussion is based on harmonic elasticity theory as described by the free energy of Eqs. (27a). We shall make frequent use of the elastic Green function, which is defined in Eqs. (31b) and computed in Appendix C. The effects of Goldstone fluctuations are most striking in two dimensions, hence the two-dimensional solid will be discussed separately in Sec. VII.

### A. Order parameter reduction due to Goldstone fluctuations

Classically, the order parameter expectation value is given by Eq. (6) or, equivalently,

$$\langle V\Omega(\mathbf{x}, k_\tau) \rangle \equiv \left\langle \int d\mathbf{k}_{\text{tot}} e^{-i\mathbf{k}_{\text{tot}} \cdot \mathbf{x}} V\Omega(k) \right\rangle \quad (33a)$$

$$= \sum_{\mathbf{k}_{\text{tot}}} e^{-i\mathbf{k}_{\text{tot}} \cdot \mathbf{x}} \langle \Omega(k) \rangle \approx \mathcal{W}(k_\tau). \quad (33b)$$

The effect of Goldstone fluctuations on the order parameter expectation value is estimated from the Gaussian theory (27a), via which we compute the mean value of the distorted classical state,

$$\langle V\Omega(\mathbf{x}, k_\tau) \rangle = \left\langle \int d\mathbf{k}_{\text{tot}} e^{-i\mathbf{k}_{\text{tot}} \cdot \mathbf{x}} V\Omega(k) \right\rangle \quad (34a)$$

$$= \sum_{\mathbf{k}_{\text{tot}}} e^{-i\mathbf{k}_{\text{tot}} \cdot \mathbf{x}} \langle \Omega(k) \rangle \quad (34b)$$

$$\approx \langle e^{ik_\tau u_\tau(\mathbf{x})} \rangle \mathcal{W}(k_\tau). \quad (34c)$$

This is readily evaluated via the Gaussian property of  $u$ , and hence we find

$$\langle V\Omega(\mathbf{x}, k_\tau) \rangle \approx \tilde{\mathcal{W}}(k_\tau), \quad (35a)$$

$$\tilde{\mathcal{W}}(k_\tau) \equiv \exp(-T\Gamma_D k_\tau^2 / 2\mu_0) \mathcal{W}(k_\tau), \quad (35b)$$

for the fluctuation-renormalized form of  $\mathcal{W}(k_\tau)$ . Here  $D\Gamma_D \equiv \mathcal{G}_{dd}(\mathbf{x})|_{\mathbf{x}=0}$  and summation over repeated Cartesian indices is implied. Recalling the classical structure for  $\mathcal{W}$ , Eq. (26a), we see that the effect of the fluctuations is to induce, in say Eq. (6) or (33b), the replacement

$$\mathcal{W}(k_\tau) = Q \int_0^\infty d\xi^2 \mathcal{N}(\xi^2) e^{-\xi^2 k_\tau^2 / 2} \rightarrow \tilde{\mathcal{W}}(k_\tau), \quad (36a)$$

$$\begin{aligned} \tilde{\mathcal{W}}(k_\tau) &\equiv e^{-T\Gamma_D k_\tau^2 / 2\mu_0} Q \int_0^\infty d\xi^2 \mathcal{N}(\xi^2) e^{-\xi^2 k_\tau^2 / 2} \\ &= Q \int_{T\Gamma_D / \mu_0}^\infty d\xi^2 \mathcal{N}(\xi^2 - (T\Gamma_D / \mu_0)) e^{-\xi^2 k_\tau^2 / 2} \\ &= Q \int_0^\infty d\xi^2 \tilde{\mathcal{N}}(\xi^2) e^{-\xi^2 k_\tau^2 / 2}, \end{aligned} \quad (36b)$$

i.e., a rigid shift of the distribution  $\mathcal{N}$  to longer (squared) localization lengths, as encoded in the new distribution  $\tilde{\mathcal{N}}$ . This is to be expected: the locally fluctuating localized objects are also subject to collective fluctuations—phonons.

This shift of  $\mathcal{N}$  is determined by the value of  $\Gamma_D$  which, as shown in Appendix C, has the following leading-order dependence on  $D$ :

$$\Gamma_D \approx \begin{cases} \frac{\Sigma_D}{(2\pi)^2} \frac{D-1}{D(D-2)} \frac{1}{\ell_{<}^{D-2}} & \text{for } D > 2, \\ \frac{1}{4\pi} \ln(\ell_{>}/\ell_{<}) & \text{for } D = 2. \end{cases} \quad (37)$$

where  $\Sigma_D$  is the area of the  $(D-1)$ -dimensional surface of a  $D$ -dimensional sphere of radius unity, viz.,

$$\Sigma_D = 2\pi^{D/2} / \Gamma(D/2), \quad (38)$$

in which  $\Gamma(D)$  [not to be confused with  $\Gamma_D$  of Eq. (37)] is the conventional gamma function. We see that in dimension  $D$  greater than two the shift is *finite*. However, at and below  $D=2$  the shift *diverges* with the long-distance cutoff  $\ell_{>}$ , viz., the linear size of the system, doing so logarithmically in two dimensions. Not surprisingly, fluctuations destroy particle localization in two-dimensional amorphous solids and thus restore the symmetry broken at the classical level (see below).

We now consider the scaling behavior of the fluctuation-induced shift of the distribution from  $\mathcal{N}$  to  $\tilde{\mathcal{N}}$ . We see from Eqs. (36) that this shift is parametrized by the length  $\xi_{\text{fl}}$ , which is defined via

$$\xi_{\text{fl}}^2 \equiv \Gamma_D T / \mu_0. \quad (39)$$

How does this length compare with the typical localization length  $\xi_{\text{typ}}$ , as defined, say, via the most probable value of  $\xi$  predicted by the classical theory? From Eq. (26c) we see that

$$\xi_{\text{typ}}^2 \sim \xi_0^2 / \tau, \quad (40)$$

and thus we have that

$$\xi_{\text{fl}}^2 / \xi_{\text{typ}}^2 \sim \Gamma_D T \tau / \mu_0 \xi_0^2. \quad (41)$$

Now, from Eq. (28c) we have that

$$\mu_0 / T \sim c\tau^3, \quad (42)$$

and we use this to eliminate  $\mu_0 / T$  in Eq. (41). Furthermore, from Eq. (37) we have that, for  $D > 2$ ,



$$\Gamma_D \sim \ell_{<}^{2-D} \sim \xi_{\text{typ}}^{2-D}, \quad (43)$$

provided we take the short-distance cutoff to be of order  $\xi_{\text{typ}}$ , as discussed in Sec. V. We use this to eliminate  $\Gamma_D$  in favor of  $\xi_{\text{typ}}$ . Finally, by using Eq. (40) to eliminate  $\tau$  in favor of  $\xi_{\text{typ}}/\xi_0$  we obtain, for  $D > 2$ ,

$$\xi_{\text{fl}}^2/\xi_{\text{typ}}^2 \sim (c\xi_0^D)^{-1}(\xi_{\text{typ}}/\xi_0)^{6-D}. \quad (44)$$

At  $D=6$  we find *one-parameter scaling* in the sense that  $\xi_{\text{fl}} \sim \xi_{\text{typ}}$ , up to the factor  $c\xi_0^D$ , which measures the number of crosslinked entities within a region of order the size of a single one. This is to be expected, because we have used classical exponents for the divergence of  $\xi_{\text{typ}}$  and vanishing of  $\mu_0$  with  $\tau$ , and six is the upper critical dimension for the transition to the amorphous solid state. In fact, if we were to replace these classical exponent by their anomalous values we would expect to recover one-parameter scaling at arbitrary  $D$ .

### B. Two-field order parameter correlations

As with their effect on the order parameter itself, the effect of Goldstone fluctuations on the two-field correlator can be determined from the Gaussian theory (27a), which gives

$$\langle V\Omega(\mathbf{x}, k_\tau) V\Omega(\mathbf{x}', k'_\tau)^* \rangle \approx \langle e^{ik_\tau u(\mathbf{x})} e^{-ik'_\tau u(\mathbf{x}')} \rangle \mathcal{W}(k_\tau) \mathcal{W}(k'_\tau). \quad (45)$$

The required correlator  $\langle \exp ik_\tau \cdot u_\tau(\mathbf{x}) \exp -ik'_\tau \cdot u_\tau(\mathbf{x}') \rangle$  is also readily evaluated via the Gaussian property of  $u$ , and hence we have

$$\begin{aligned} & \langle V\Omega(\mathbf{x}, k_\tau) V\Omega(\mathbf{x}', k'_\tau)^* \rangle \\ & \approx \exp\left(-\frac{T\Gamma_D}{2\mu_0} |k_\tau - k'_\tau|^2\right) \exp\left(-\frac{T}{\mu_0} (\mathcal{G}_{dd'}(\mathbf{0}) \right. \\ & \quad \left. - \mathcal{G}_{dd'}(\mathbf{x} - \mathbf{x}')) k_{\tau d} \cdot k'_{\tau d'}\right) \mathcal{W}(k_\tau) \mathcal{W}(k'_\tau), \quad (46) \end{aligned}$$

where the scalar products  $k_{\tau d} \cdot k'_{\tau d'}$  and  $|k_\tau - k'_\tau|^2$  are, respectively, taken over  $n$  and  $nD$  components. Recall, from Eq. (37), that  $\Gamma_D|_{D=2}$  diverges with the long-distance cutoff. This, together with the positive-semidefiniteness of the quadratic form  $[\mathcal{G}_{dd'}(\mathbf{0}) - \mathcal{G}_{dd'}(\mathbf{x} - \mathbf{x}')] k_{\tau d} \cdot k'_{\tau d'}$  in Eq. (46), makes it evident that the correlator  $\langle V\Omega(\mathbf{x}, k_\tau) V\Omega(\mathbf{x}', k'_\tau)^* \rangle$  given in Eq. (46) vanishes at  $D=2$  (and below) unless  $k=k'$ . This vanishing is a second facet of the fluctuation-induced restoration of symmetry discussed for the case of the order parameter, following Eq. (37). [The correlator  $\langle V\Omega(k) V\Omega(k')^* \rangle$  vanishes in *any* dimension unless  $k_\lambda = k'_\lambda$ , owing to the preserved symmetry of common translations of the replicas, which encodes the homogeneity of the randomness in the amorphous solid state, i.e., its macroscopic translational invariance.] If  $k=k'$  then, regardless of dimension, the correlator decays with increasing separation  $\mathbf{x} - \mathbf{x}'$ , as shown by Eq. (46).

For  $D > 2$  it is convenient to analyze the two-field correlator normalized by its disconnected part, i.e.,

$$\frac{\langle \Omega(\mathbf{x}, k_\tau) \Omega(\mathbf{x}', k'_\tau)^* \rangle}{\langle \Omega(\mathbf{x}, k_\tau) \rangle \langle \Omega(\mathbf{x}', k'_\tau)^* \rangle}. \quad (47)$$

Equations (46) and (35) show this quotient to be given by

$$\exp\left(\frac{T}{\mu_0} \mathcal{G}_{dd'}(\mathbf{r}) k_{\tau d} \cdot k'_{\tau d'}\right), \quad (48)$$

where the separation  $\mathbf{r} \equiv \mathbf{x} - \mathbf{x}'$ .

We illustrate this behavior by considering the case of  $D=3$  and the regime  $\ell_{<} \ll |\mathbf{r}| \ll \ell_{>}$ , for which, as shown in Appendix C (see also, e.g., Ref. 8), we may use

$$\mathcal{G}_{dd'}^{(3)}(\mathbf{r}) \approx \frac{1}{8\pi|\mathbf{r}|} (\delta_{dd'} + \hat{r}_d \hat{r}_{d'}), \quad (49)$$

where the unit vector  $\hat{\mathbf{r}} \equiv \mathbf{r}/|\mathbf{r}|$ , and by choosing  $k=k' = \{\mathbf{0}, \mathbf{q}, -\mathbf{q}, \mathbf{0}, \dots, \mathbf{0}\}$ . Then in this regime the normalized two-field correlator is given by

$$\exp\left(\frac{T}{4\pi\mu_0} \frac{|\mathbf{q}|^2}{|\mathbf{r}|} (1 + \cos^2 \varphi)\right), \quad (50)$$

which depends strongly on the angle  $\varphi$  between the vectors  $\mathbf{q}$  and  $\mathbf{r}$ .

We may also examine the normalized two-field correlator in the regime  $|\mathbf{r}| \ll \ell_{<}$ . Making use of  $\mathcal{G}_{dd'}^{(3)}(\mathbf{r})$  in this regime, as given in Eq. (C10) of Appendix C, we find that the normalized two-field correlator is given by

$$\exp\left(\frac{4T}{3\pi\mu_0} \frac{|\mathbf{q}|^2}{\ell_{<}}\right) \exp\left(\frac{2T}{45\pi\mu_0} \frac{|\mathbf{q}|^2 |\mathbf{r}|^2}{\ell_{<}^2} (-2 + \cos^2 \varphi)\right), \quad (51)$$

where  $\ell_{<} \equiv \ell_{<}/2\pi$  (and  $\ell_{>} \equiv \ell_{>}/2\pi$ ). Of course, in this regime the result for the correlator is incomplete, as there will also be contributions from the non-Goldstone excitations.

### C. Intermezzo on length scales

We pause to catalog the various length scales featured in the present paper, and to indicate where they first appear.

The shortest length is  $\ell_p$ , the persistence length of a macromolecule, which appears alongside  $L$ , the arclength of a macromolecule, shortly after Eq. (23). Together, they yield  $\xi_0$ , the linear size of the objects being linked, which may be substantially larger than  $\ell_p$ . It is only through  $\xi_0$  that  $\ell_p$  and  $L$  feature in the free energy, Eq. (23). The density  $c$  of entities being constrained also first features in Eq. (23), and sets a length scale,  $c^{-1/D}$ , in Eq. (44). Comparable to or longer than  $\xi_0$  is the length  $\xi$ , the (distributed) localization length, first featuring in Eqs. (2) and (3). The typical value of  $\xi$  is denoted  $\xi_{\text{typ}}$ , first mentioned around Eq. (40). The amount by which fluctuations shift the distribution of  $\xi$  is encoded in the fluctuation length  $\xi_{\text{fl}}$ , first mentioned around Eq. (39). The short- and long-distance cutoffs for the Goldstone-type fluctuations are, respectively, denoted  $\ell_{<}$  and  $\ell_{>}$ , and are first mentioned in Sec. V. The linear size of the sample is denoted  $\mathcal{L}$ ; see the beginning of Sec. VII.

## VII. AMORPHOUS SOLIDS IN TWO DIMENSIONS

We now focus on amorphous solids in *two* dimensions. By taking the long-distance cutoff  $\ell_>$  to be the linear size of the sample  $\mathcal{L}$ , so that its area is  $\mathcal{L}^2$ , we see from Eqs. (35) and (37) that the expectation value of the order parameter does indeed *vanish algebraically* with the sample size, doing with an exponent that depends, inter alia, on  $k_\tau$ ,

$$\begin{aligned} \langle \mathcal{L}^2 \Omega(\mathbf{x}, k_\tau) \rangle &\approx \mathcal{W}(k_\tau) \exp\left(-\frac{1}{2} \eta(k_\tau^2) \ln(\mathcal{L}/\ell_<)\right) \\ &= \mathcal{W}(k_\tau) (\mathcal{L}/\ell_<)^{-\eta(k_\tau^2)/2}, \end{aligned} \quad (52)$$

where the exponent  $\eta(\kappa^2)$  varies continuously with wave number and is defined via

$$\eta(\kappa^2) \equiv \frac{T\kappa^2}{4\pi\mu_0}. \quad (53)$$

To arrive at this result we have made use of the two-dimensional real-space elastic Green function evaluated at the origin, computed in Appendix C and stated in Eq. (37). It confirms the expectation, mentioned above, that in two dimensions fluctuations destroy particle localization and restore the broken symmetry. Note, however that, due to the purely entropic nature of the elasticity the exponent does not depend on temperature [cf. Eq. (28c)].

Similarly, from Eq. (46) we see that the  $k_\tau$ -diagonal two-field correlator is given by

$$\begin{aligned} \langle \mathcal{L}^2 \Omega(\mathbf{x}, k_\tau) \mathcal{L}^2 \Omega(\mathbf{x}', k_\tau) \rangle & \\ \approx \mathcal{W}(k_\tau)^2 \exp\left(-\frac{T}{\mu_0} (\mathcal{G}_{dd'}(\mathbf{0}) - \mathcal{G}_{dd'}(\mathbf{r})) k_{\tau d} \cdot k_{\tau d'}\right), \end{aligned} \quad (54)$$

where, as before, the separation is denoted by  $\mathbf{r} \equiv \mathbf{x} - \mathbf{x}'$  and the unit vector by  $\hat{\mathbf{r}} \equiv \mathbf{r}/|\mathbf{r}|$ . In the regime  $\ell_< \ll |\mathbf{r}| \ll \mathcal{L}$ , the Green function is given by [see Eq. (C28) in Appendix C]

$$\mathcal{G}_{dd'}(\mathbf{0}) - \mathcal{G}_{dd'}(\mathbf{r}) = \frac{1}{4\pi} \{\delta_{dd'} \ln(r/\ell_<) - \hat{r}_d \hat{r}_{d'}\}, \quad (55)$$

where, for convenience, we have introduced the numerically rescaled short-distance cutoff  $\tilde{\ell}_<$ , defined via

$$\tilde{\ell}_< \equiv \frac{\ell_<}{\pi e^{\gamma + \frac{1}{2}}}. \quad (56)$$

In consequence, the correlator decays algebraically with the *magnitude*  $r$  of the distance, and with an amplitude that depends on the *orientation*  $\hat{\mathbf{r}}$  of the distance (relative to  $k_\tau$ ). Ignoring, for the moment the dependence on  $\hat{\mathbf{r}}$ , we have the leading-order result,

$$\langle \mathcal{L}^2 \Omega(\mathbf{x}, k_\tau) \mathcal{L}^2 \Omega(\mathbf{x}', k_\tau) \rangle \approx \mathcal{W}(k_\tau)^2 (\tilde{\ell}_</r)^2 \eta(k_\tau^2). \quad (57)$$

As mentioned above, the  $k_\tau$ -off-diagonal two-field correlator—like the order parameter—vanishes in the thermodynamic limit, reflecting the fluctuation-induced restoration of symmetry.

This scenario is similar to the theory of two-dimensional regular solids, taking into account harmonic phonons only, as

discussed in Ref. 12. The main difference is the absence of Bragg peaks at reciprocal lattice vectors. Instead, there is a divergence in the scattering function<sup>12</sup> at zero wave number, as can be seen from the Fourier transform of the correlator (57) with respect to  $\mathbf{r}$  ( $\equiv \mathbf{x} - \mathbf{x}'$ ),

$$\begin{aligned} S(\mathbf{q}, k_\tau) &= \int d\mathbf{r} e^{i\mathbf{r}\cdot\mathbf{q}} \langle \mathcal{L}^2 \Omega(\mathbf{x}, k_\tau) \mathcal{L}^2 \Omega(\mathbf{x}', k_\tau) \rangle \\ &= \mathcal{W}(k_\tau)^2 \ell_<^2 \left\{ \left( \frac{\ell_>}{\ell_<} \right)^{2-\eta} \frac{J_1(q\ell_>)}{q\ell_>} + B(\eta) (q\ell_<)^{\eta-2} \right\}, \\ B(x) &\equiv 2^{-x} \frac{x\Gamma(1-x/2)}{\Gamma(1+x/2)}. \end{aligned} \quad (58)$$

In these formulas,  $J_1$  denotes a Bessel function and we have abbreviated  $\eta(k_\tau^2)$  as  $\eta$ . One needs to keep the two exhibited terms because there is an exchange of dominance as  $\eta$  passes through the value  $1/2$ , i.e., at  $k_\tau^2 = 2\pi\mu_0/T$ . Specifically, for  $(\ell_>/\ell_<) \rightarrow \infty$  at fixed  $q\ell_<$  the dimensionless factor  $\{\dots\}$  behaves as

$$(q\ell_<)^{-3/2} (\ell_>/\ell_<)^{1/2-\eta} \text{ for } \eta < 1/2, \quad (59a)$$

$$(q\ell_<)^\eta \text{ for } \eta > 1/2. \quad (59b)$$

Restoring the dependence on orientation  $\hat{\mathbf{r}}$ , we arrive at the full, anisotropic form for the decay of the two-field correlator,

$$\mathcal{W}(k_\tau)^2 (\tilde{\ell}_</r)^{\eta(k_\tau^2)} \exp(\eta(k_\tau^2) \hat{k}_{\tau d} \cdot \hat{k}_{\tau d'} \hat{r}_{d_1} \hat{r}_{d_2}). \quad (60)$$

Here, the symbol  $\hat{k}_{\tau d}$  indicates the unit vector  $k_{\tau d}/|k_\tau|$ . For the illustrative case of  $k = (\mathbf{0}, \mathbf{q}, -\mathbf{q}, \mathbf{0}, \dots)$  this correlator reduces to

$$\mathcal{W}(\sqrt{2}|\mathbf{q}|)^2 (\tilde{\ell}_</r)^{2\eta(q^2)} \exp(2\eta(q^2) \cos^2 \varphi), \quad (61)$$

where, once again,  $\varphi$  is the angle between  $\mathbf{q}$  and  $\mathbf{r}$ .

The framework adopted in the present paper allows the identification of the *quasilocalized fraction*  $\bar{Q}$ , i.e., the fraction of particles that, while not truly localized, have RMS displacements that diverge only logarithmically, as the system size  $\mathcal{L}$  goes to infinity. This fraction should be contrasted with the delocalized fraction, i.e., the fractions that have RMS displacements that diverge linearly with  $\mathcal{L}$ . One way to extract the quasilocalized fraction is via the order parameter (52)—specifically the amplitude of its power-law decay with  $\mathcal{L}$ . A simpler route is via the two-field correlator (60),

$$\bar{Q}^2 = \lim_{k_\tau \rightarrow 0} \lim_{r \rightarrow \infty} (\tilde{\ell}_</r)^{-\eta(k_\tau^2)} \langle \mathcal{L}^2 \Omega(\mathbf{x}, k_\tau) \mathcal{L}^2 \Omega(\mathbf{x}', k_\tau) \rangle = \mathcal{W}(0)^2. \quad (62)$$

The option of analyzing the quasilocalized fraction would not be available to percolation-based approaches to vulcanized matter, as such approaches do not account for the thermal motion of the constituents (e.g., macromolecules), but only the architecture of the structures they constitute. In fact, for the same reason, the entire circle of ideas described in the present paper lie beyond the reach of percolation-based ap-

proaches. This shows up especially vividly in the context of the vulcanization transition in low (and especially two) dimensions. Whereas percolation theory would indicate a lower critical dimension of unity, with nothing fundamentally new happening as one reduces the dimensionality through two, the present approach correctly finds a lower critical dimension at two dimensions for the amorphous solidification transition. This is because, in addition to incorporating the physics of percolation,<sup>14,15</sup> this approach contains the logically independent physics of localization and the attendant issue of the spontaneous breaking of translational symmetry. Thus, there are qualitative, and not merely quantitative, distinctions between the vulcanization transition and resulting quasiamorphous solid state in two- and in higher-dimensional settings, owing to the strong role played by Goldstone-type fluctuations in reduced dimensions.

The results discussed in the present section echo those found for a variety of two-dimensional statistical-mechanical systems (for a survey see, e.g., Ref. 13), in the following sense. A sufficient density of random constraints triggers a phase transition from a liquid state to a quasiamorphous solid state. In the liquid state there are no clusters of constituents that span the system (i.e., the system does not percolate), there are no quasilocalized particles, order-parameter correlations decay exponentially with distance, and the static shear modulus is zero. In the solid state a cluster does span the system (i.e., percolates), there are quasilocalized particles, the static shear modulus is nonzero, and order-parameter correlations decay algebraically, with a continuously varying exponent  $\eta$  that depends, inter alia, on the scale set by the *probe wave vector*  $k_\tau$ . However, the true long-range order found in higher dimensions, fails to set in, albeit only just, due to thermal fluctuations.

The situation is reminiscent of that found in the setting of the melting of two-dimensional crystals, triggered not by the density of constraints, but rather by thermal fluctuations. In this setting, at high temperatures one has a nonrigid phase with exponentially decaying positional correlations associated with unbound dislocations. This is the analog of the nonpercolating state of quasiamorphous solids. At lower temperatures one has a rigid phase, associated with bound dislocations and algebraically decaying positional correlations, but no true long-range positional order. This is the analog of the percolating regime of amorphous solids. The permanence of the architecture of the amorphous solid forming systems discussed in the present paper prohibits the destruction by thermal fluctuations of a percolating raft of constituents. However, percolation does not enforce true localization.

In two-dimensional crystallization one also has the opportunity for correlations in the *orientations* of the bonds connecting neighboring particles. Thus, at low temperatures one has, in addition to quasilong range positional correlations, true long-range orientational correlations. This brings the opportunity for an intermediate regime of temperatures, in which dislocations are unbound but disclinations, which would disrupt the orientational order, remain bound: the hexatic phase of two-dimensional crystals.

This opportunity does not seem to be present in the model of vulcanized matter discussed here, which focuses exclusively on positional order and does not support topological excitations. Richer settings, such as those involving macromolecules with liquid crystalline degrees of freedom, seem likely to raise interesting opportunities for order in low-dimensional random systems.

## VIII. PHYSICAL CONTENT OF CORRELATORS

### A. Identifying the statistical information in the two-field correlator

What is the meaning of the correlators in the amorphous solid state of the vulcanization field theory? Let us begin with the two-field correlator  $\langle \Omega(k_1)\Omega(k_2)^* \rangle$ . Specializing to the case in which the zero-replica entries  $\mathbf{k}_1^0$  and  $\mathbf{k}_2^0$  are zero, the interpretation of this replica quantity is given by

$$\langle \Omega(k_1)\Omega(k_2)^* \rangle |_{\mathbf{k}_1^0=\mathbf{k}_2^0=0} = \left[ \frac{1}{J^2} \sum_{j_1, j_2=1}^J \prod_{\alpha=1}^n \langle e^{i\mathbf{k}_1^\alpha \cdot \mathbf{R}_{j_1}} - i\mathbf{k}_2^\alpha \cdot \mathbf{R}_{j_2} \rangle \right], \quad (63)$$

which expresses the connection with the (semimicroscopic) correlators of all pairs of particles that constitute the system. Consider a simple illustrative example, in which the positions of pairs of localized particles fluctuate about their mean positions according to a general Gaussian correlated distribution. For such particles we would then have

$$\begin{aligned} \langle e^{i\mathbf{k}_1 \cdot \mathbf{R}_{j_1} - i\mathbf{k}_2 \cdot \mathbf{R}_{j_2}} \rangle &= e^{i\mathbf{k}_1 d_{j_1} - i\mathbf{k}_2 d_{j_2}} e^{-\frac{1}{2} \Delta r_{j_1 j_1 d_1 d_2} k_{1d_1} k_{1d_2}} \\ &\quad \times e^{-\frac{1}{2} \Delta r_{j_2 j_2 d_1 d_2} k_{2d_1} k_{2d_2}} e^{\Delta r_{j_1 j_2 d_1 d_2} k_{1d_1} k_{2d_2}}, \end{aligned} \quad (64)$$

where the mean, variances ( $j_1=j_2$ ) and covariances ( $j_1 \neq j_2$ ) of the positions are given by

$$\mathbf{r}_j = \langle \mathbf{R}_j \rangle, \quad (65a)$$

$$\Delta r_{j_1 j_2 d_1 d_2} = \langle (R_{j_1 d_1} - \langle R_{j_1 d_1} \rangle)(R_{j_2 d_2} - \langle R_{j_2 d_2} \rangle) \rangle, \quad (65b)$$

and summations over repeated Cartesian indices  $d_1$  and  $d_2$  are implied.

Setting such contributions together from all pairs of *localized*, particles we have

$$\begin{aligned} \langle \Omega(k_1)\Omega(k_2)^* \rangle |_{\mathbf{k}_1^0=\mathbf{k}_2^0=0} &= Q^2 \int d\hat{\mathbf{r}}_1 d\hat{\mathbf{r}}_2 d\hat{\Delta}r_{11} d\hat{\Delta}r_{22} d\hat{\Delta}r_{12} \\ &\quad \times \mathcal{P}(\hat{\mathbf{r}}_1, \hat{\mathbf{r}}_2, \hat{\Delta}r_{11}, \hat{\Delta}r_{22}, \hat{\Delta}r_{12}) e^{i\hat{r}_{1d} \sum_{\alpha=1}^n k_{1d}^\alpha - i\hat{r}_{2d} \sum_{\alpha=1}^n k_{2d}^\alpha} \\ &\quad \times e^{-1/2 \hat{\Delta}r_{11 d_1 d_2} \sum_{\alpha=1}^n k_{1d_1}^\alpha k_{1d_2}^\alpha} e^{-1/2 \hat{\Delta}r_{22 d_1 d_2} \sum_{\alpha=1}^n k_{2d_1}^\alpha k_{2d_2}^\alpha} \\ &\quad \times e^{\hat{\Delta}r_{12 d_1 d_2} \sum_{\alpha=1}^n k_{1d_1}^\alpha k_{2d_2}^\alpha}, \end{aligned} \quad (66)$$

$$\begin{aligned} & \mathcal{P}(\hat{\mathbf{r}}_1, \hat{\mathbf{r}}_2, \hat{\Delta}r_{11}, \hat{\Delta}r_{22}, \hat{\Delta}r_{12}) \\ & \equiv \left[ \frac{1}{(QJ)^2} \sum_{j_1, j_2 \text{ loc}} \delta(\hat{\mathbf{r}}_1 - \mathbf{r}_{j_1}) \delta(\hat{\mathbf{r}}_2 - \mathbf{r}_{j_2}) \delta(\hat{\Delta}r_{11} - \Delta r_{j_1 j_1}) \right. \\ & \quad \left. \times \delta(\hat{\Delta}r_{22} - \Delta r_{j_2 j_2}) \delta(\hat{\Delta}r_{12} - \Delta r_{j_1 j_2}) \right], \end{aligned}$$

where we have introduced  $\mathcal{P}$ , the disorder-averaged joint distribution, over the pairs of localized particles, of the means, variances and covariances of the particle positions. The macroscopic translational invariance of the amorphous solid state ensures that  $\mathcal{P}$  depends on  $\hat{\mathbf{r}}_1$  and  $\hat{\mathbf{r}}_2$  only through their difference, and thus we replace  $\mathcal{P}$  by  $V^{-1}\mathcal{P}(\hat{\mathbf{r}}_1 - \hat{\mathbf{r}}_2, \hat{\Delta}r_{11}, \hat{\Delta}r_{22}, \hat{\Delta}r_{12})$ . By appealing to permutation symmetry, including the zeroth replica, we can reinstate the dependence on the zeroth-replica wave vectors, and hence arrive at a hypothesized form for the two-point correlator,

$$\begin{aligned} & \langle \Omega(k_1) \Omega(k_2) \rangle^* \\ & = Q^2 \int d\hat{\mathbf{r}}_1 d\hat{\mathbf{r}}_2 d\hat{\Delta}r_{11} d\hat{\Delta}r_{22} d\hat{\Delta}r_{12} V^{-1} \\ & \quad \times \mathcal{P}(\hat{\mathbf{r}}_1 - \hat{\mathbf{r}}_2, \hat{\Delta}r_{11}, \hat{\Delta}r_{22}, \hat{\Delta}r_{12}) e^{i\hat{r}_{1d} \sum_{\alpha=0}^n k_{1d}^\alpha - i\hat{r}_{2d} \sum_{\alpha=0}^n k_{2d}^\alpha} \\ & \quad \times e^{-1/2 \hat{\Delta}r_{11d_1 d_2} \sum_{\alpha=0}^n k_{1d_1}^\alpha k_{1d_2}^\alpha} e^{-1/2 \hat{\Delta}r_{22d_1 d_2} \sum_{\alpha=0}^n k_{2d_1}^\alpha k_{2d_2}^\alpha} \\ & \quad \times e^{\hat{\Delta}r_{12d_1 d_2} \sum_{\alpha=0}^n k_{1d_1}^\alpha k_{2d_2}^\alpha}. \end{aligned} \quad (67)$$

What about contributions to the double sum over particles in Eq. (63) associated with one or two *unlocalized* particles? Such contributions certainly exist, except in the limit of large cross-link densities (where all constituents are bound to the infinite cluster and are, therefore, localized); in the liquid state they would, of course, be the only contributions. There, they would give rise to *diagonal* contributions, i.e., the correlator  $\langle \Omega(k_1) \Omega(k_2) \rangle^*$  would vanish unless  $k_1 = k_2$ , owing to the intact symmetry of independent translations of the replicas. In the solid state, contributions associated with unlocalized particles are expected to give rise to short-ranged correlations. As such correlations are not the main focus of the present paper, we neglect contributions to the two-field correlator associated with unlocalized particles.

### B. Evaluating the statistical information in the two-field correlator

In Sec. VIII A we have connected the two-field correlator  $\langle V\Omega(k) V\Omega(k') \rangle^*$  to the distribution  $\mathcal{P}$  that characterizes pairs of localized particles [see Eq. (67)], and in Sec. VI B we have evaluated the Fourier transform of this correlator,  $\langle V\Omega(\mathbf{x}, k_\tau) V\Omega(\mathbf{x}', k'_\tau) \rangle^*$ , within the Goldstone-type fluctuation approach [see Eq. (46)]. We now discuss the implications of resulting correlator for the properties of the distribution.

To do this, it is convenient to exchange the correlator in Eq. (46) for the Fourier transform,

$$\begin{aligned} & \langle \Omega(k) \Omega(k') \rangle^* \\ & = \int \frac{d\mathbf{x} d\mathbf{x}'}{V} e^{i\mathbf{k}_{\text{tot}} \cdot \mathbf{x}} e^{-i\mathbf{k}'_{\text{tot}} \cdot \mathbf{x}'} \langle V\Omega(\mathbf{x}, k_\tau) V\Omega(\mathbf{x}', k'_\tau) \rangle^* \\ & \approx \tilde{\mathcal{W}}(k_\tau) \tilde{\mathcal{W}}(k'_\tau) \int \frac{d\mathbf{x} d\mathbf{x}'}{V} e^{i\mathbf{k}_{\text{tot}} \cdot \mathbf{x}} e^{-i\mathbf{k}'_{\text{tot}} \cdot \mathbf{x}'} \\ & \quad \times \exp\left(\frac{T}{\mu_0} \mathcal{G}_{dd'}(\mathbf{x} - \mathbf{x}') k_{\tau d} \cdot k'_{\tau d'}\right) \\ & = \tilde{\mathcal{W}}(k_\tau) \tilde{\mathcal{W}}(k'_\tau) \delta_{\mathbf{k}_{\text{tot}}, \mathbf{k}'_{\text{tot}}} \int \frac{d\mathbf{x}}{V} e^{i\mathbf{k}_{\text{tot}} \cdot \mathbf{x}} \\ & \quad \times \exp\left(\frac{T}{\mu_0} \mathcal{G}_{dd'}(\mathbf{x}) k_{\tau d} \cdot k'_{\tau d'}\right), \end{aligned} \quad (68)$$

where  $\tilde{\mathcal{W}}(k_\tau)$  is the fluctuation-renormalized order parameter given in Eqs. (35b) and (36b). Next, in Eq. (67) we perform the integration over the center of mass of  $\mathbf{r}_1$  and  $\mathbf{r}_2$ , and equate the resulting form of the correlator to the form given in Eq. (68), having dropped the hats on the dummy variables, thus arriving at a formula obeyed by the distribution  $\mathcal{P}$ ,

$$\begin{aligned} & Q^2 \delta_{\mathbf{k}_1 \text{ tot}, \mathbf{k}_2 \text{ tot}} \int d\mathbf{x} d\Delta r_{11} d\Delta r_{22} d\Delta r_{12} \mathcal{P}(\mathbf{x}, \Delta r_{11}, \Delta r_{22}, \Delta r_{12}) \\ & \quad \times e^{i\mathbf{k}_1 \text{ tot} \cdot \mathbf{x}} e^{-1/2 \Delta r_{11d_1 d_2} \sum_{\alpha=0}^n k_{1d_1}^\alpha k_{1d_2}^\alpha} e^{-1/2 \Delta r_{22d_1 d_2} \sum_{\alpha=0}^n k_{2d_1}^\alpha k_{2d_2}^\alpha} \\ & \quad \times e^{\Delta r_{12d_1 d_2} \sum_{\alpha=0}^n k_{1d_1}^\alpha k_{2d_2}^\alpha} \\ & = \tilde{\mathcal{W}}(k_{1\tau}) \tilde{\mathcal{W}}(k_{2\tau}) \delta_{\mathbf{k}_1 \text{ tot}, \mathbf{k}_2 \text{ tot}} \int \frac{d\mathbf{x}}{V} e^{i\mathbf{k}_1 \text{ tot} \cdot \mathbf{x}} \\ & \quad \times \exp\left(\frac{T}{\mu_0} \mathcal{G}_{d_1 d_2}(\mathbf{x}) k_{1\tau d_1} \cdot k_{2\tau d_2}\right). \end{aligned} \quad (69)$$

By solving this equation for  $\mathcal{P}(\mathbf{x}, \Delta r_{11}, \Delta r_{22}, \Delta r_{12})$  one learns that it has weight only at values of  $(\Delta r_{11}, \Delta r_{22}, \Delta r_{12})$  of the form  $(\xi_1^2 \mathbb{1}, \xi_1^2 \mathbb{1}, (T/\mu_0) \mathcal{G}_{d_1 d_2}(\mathbf{y}))$  for some values of the parameters  $(\xi_1, \xi_1, \mathbf{y})$ , where  $\mathbb{1}$  is the identity in  $D$ -dimensional Cartesian space. Anticipating this, it is convenient to introduce the following parametrization in terms of a reduced distribution  $\mathcal{P}(\mathbf{x}, \xi_1^2, \xi_2^2, \mathbf{y})$ :

$$\begin{aligned} & \mathcal{P}(\mathbf{x}, \Delta r_{11}, \Delta r_{22}, \Delta r_{12}) \\ & = \int d\xi_1^2 \tilde{\mathcal{N}}(\xi_1^2) d\xi_2^2 \tilde{\mathcal{N}}(\xi_2^2) \delta(\Delta r_{11} - \xi_1^2 \mathbb{1}) \delta(\Delta r_{22} - \xi_2^2 \mathbb{1}) \\ & \quad \times \int \frac{d\mathbf{y}}{V} \delta(\Delta r_{12} - (T/\mu_0) \mathcal{G}(\mathbf{y})) \mathcal{P}(\mathbf{x}, \xi_1^2, \xi_2^2, \mathbf{y}). \end{aligned} \quad (70)$$

Note that  $\mathcal{P}(\mathbf{x}, \xi_1^2, \xi_2^2, \mathbf{y})$  only becomes a true distribution when an appropriate Jacobian factor associated with the  $\mathbf{y}$  dependence is introduced; nevertheless we shall continue to refer to it as a distribution. As shown in Appendix D, Eq. (69) can be solved for the reduced probability distribution; the solution is given in Eq. (D9). Thus one finds for the full distribution,

$$\begin{aligned}
& \mathcal{P}(\mathbf{x}, \Delta r_{11}, \Delta r_{22}, \Delta r_{12}) \\
&= \int d\xi_1^2 \tilde{\mathcal{N}}(\xi_1^2) d\xi_2^2 \tilde{\mathcal{N}}(\xi_2^2) \delta(\Delta r_{11} - \xi_1^2) \delta(\Delta r_{22} - \xi_2^2) \\
&\quad \times \int \frac{d\mathbf{y}}{V} \left\{ \int d\mathbf{q} e^{-i\mathbf{q}\cdot(\mathbf{x}-\mathbf{y})} \exp\left(\frac{1}{2}(\xi_1^2 + \xi_2^2)q^2 \right. \right. \\
&\quad \left. \left. - \Delta r_{12d_1d_2} q_{d_1} q_{d_2} \right) \right\} \delta[\Delta r_{12} - (T/\mu_0)\mathcal{G}(\mathbf{y})]. \quad (71)
\end{aligned}$$

This has the structure of a source term, associated with the range of values of  $\mathcal{G}$ , convoluted with an appropriate ‘‘propagator.’’

It should be borne in mind that, in this solution for the full distribution, Eq. (71), the integration over wave vectors  $\mathbf{q}$  is subject to the usual cutoffs, i.e., those featured in Eq. (31b). Thus, even though the exponent in the factor  $\exp[\frac{1}{2}(\xi_1^2 + \xi_2^2)q^2 - \Delta r_{12d_1d_2} q_{d_1} q_{d_2}]$  grows at large  $\mathbf{q}$  (i.e., the factor is *not* a decaying Gaussian factor), the large-wave-vector cutoff protects against divergence. In fact, if we focus on the distribution  $\mathcal{P}$  at separations  $\mathbf{x}$  that are large compared with the cutoff  $\ell_<$  then for values of  $\xi_1$  and  $\xi_2$  with appreciable weight the aforementioned exponent is small, and we may expand to obtain

$$\begin{aligned}
& \mathcal{P}(\mathbf{x}, \Delta r_{11}, \Delta r_{22}, \Delta r_{12}) \\
&= \int d\xi_1^2 \tilde{\mathcal{N}}(\xi_1^2) d\xi_2^2 \tilde{\mathcal{N}}(\xi_2^2) \delta(\Delta r_{11} - \xi_1^2) \delta(\Delta r_{22} - \xi_2^2) \\
&\quad \times \exp\left(-\frac{1}{2}(\xi_1^2 + \xi_2^2)\nabla_{\mathbf{x}}^2 + \Delta r_{12d_1d_2} \partial_{d_1} \partial_{d_2}\right) \\
&\quad \times \int \frac{d\mathbf{y}}{V} \tilde{\delta}(\mathbf{x} - \mathbf{y}) \delta(\Delta r_{12} - (T/\mu_0)\mathcal{G}(\mathbf{y})) \quad (72a)
\end{aligned}$$

$$\begin{aligned}
& \approx \int d\xi_1^2 \tilde{\mathcal{N}}(\xi_1^2) d\xi_2^2 \tilde{\mathcal{N}}(\xi_2^2) \delta(\Delta r_{11} - \xi_1^2) \delta(\Delta r_{22} - \xi_2^2) \\
&\quad \times \frac{1}{V} \exp\left(-\frac{1}{2}(\xi_1^2 + \xi_2^2)\nabla_{\mathbf{x}}^2 + \Delta r_{12d_1d_2} \partial_{d_1} \partial_{d_2}\right) \delta \\
&\quad \times (\Delta r_{12} - (T/\mu_0)\mathcal{G}(\mathbf{x})) \quad (72b)
\end{aligned}$$

$$\begin{aligned}
& \approx \int d\xi_1^2 \tilde{\mathcal{N}}(\xi_1^2) d\xi_2^2 \tilde{\mathcal{N}}(\xi_2^2) \delta(\Delta r_{11} - \xi_1^2) \delta(\Delta r_{22} - \xi_2^2) \\
&\quad \times \frac{1}{V} \left\{ 1 - \frac{1}{2}(\xi_1^2 + \xi_2^2)\nabla_{\mathbf{x}}^2 + \Delta r_{12d_1d_2} \partial_{d_1} \partial_{d_2} \right\} \\
&\quad \times \delta(\Delta r_{12} - (T/\mu_0)\mathcal{G}(\mathbf{x})). \quad (72c)
\end{aligned}$$

Here,  $\partial_d \equiv \partial/\partial x_d$ , and  $\tilde{\delta}$  indicates the smoothed delta function resulting from the application of the wave-vector cutoff to the Fourier integration that yields it. We have, however, proceeded to the second and third lines without explicitly indicating the effect of this smoothing, viz., the replacement of the factor  $\delta[\Delta r_{12} - (T/\mu_0)\mathcal{G}(\mathbf{x})]$  the same quantity *smear*ed over a region around the point  $\mathbf{x}$  having linear dimension of order the short-distance cutoff.

### C. Two- (and higher-) field correlators as distributions of particle correlations

Let us pause to revisit the interpretation of the two-field correlator. To do this, we introduce the disorder-averaged distribution  $\mathcal{M}_2$  of two-particle correlators  $\mathcal{C}$ , viz.,

$$\mathcal{M}_2[\mathcal{C}] \equiv \left[ J^{-2} \sum_{j_1, j_2=1}^J \prod_{\mathbf{k}_1, \mathbf{k}_2 \neq \mathbf{0}} \delta_c(\mathcal{C}_{\mathbf{k}_1 \mathbf{k}_2} - \langle e^{i\mathbf{k}_1 \cdot \mathbf{R}_{j_1} + i\mathbf{k}_2 \cdot \mathbf{R}_{j_2}} \rangle) \right], \quad (73)$$

in which  $\delta_c(x+iy) \equiv \delta(x)\delta(y)$ . We can then observe that the two-field correlator, Eq. (63), can be expressed as a suitable moment of  $\mathcal{M}_2$ ,

$$\langle \Omega(k_1)\Omega(k_2) \rangle = \int \mathcal{DC} \mathcal{M}_2[\mathcal{C}] \prod_{\alpha=0}^n \mathcal{C}_{\mathbf{k}_1 \mathbf{k}_2}^{\alpha}. \quad (74)$$

Note that we have appealed to replica permutation symmetry in order to reinstate the dependence on the zeroth-replica wave vectors.

It is straightforward to extend this discussion to the general case of  $r$ -particle correlators  $\langle e^{i\mathbf{k}_1 \cdot \mathbf{R}_{j_1} + i\mathbf{k}_2 \cdot \mathbf{R}_{j_2} + \dots + i\mathbf{k}_r \cdot \mathbf{R}_{j_r}} \rangle$ , for which the distribution  $\mathcal{M}_r$  is given by

$$\begin{aligned}
\mathcal{M}_r[\mathcal{C}] \equiv & \left[ \frac{1}{J^r} \sum_{j_1, \dots, j_r=1}^J \prod_{\mathbf{k}_1, \mathbf{k}_2, \dots, \mathbf{k}_r \neq \mathbf{0}} \delta_c(\mathcal{C}_{\mathbf{k}_1 \mathbf{k}_2 \dots \mathbf{k}_r} \right. \\
& \left. - \langle e^{i\mathbf{k}_1 \cdot \mathbf{R}_{j_1} + i\mathbf{k}_2 \cdot \mathbf{R}_{j_2} + \dots + i\mathbf{k}_r \cdot \mathbf{R}_{j_r}} \rangle) \right]. \quad (75)
\end{aligned}$$

Observe that the  $r$ -field correlator can also be expressed as a suitable moment,

$$\langle \Omega(k_1)\Omega(k_2) \dots \Omega(k_r) \rangle = \int \mathcal{DC} \mathcal{M}_r[\mathcal{C}] \prod_{\alpha=0}^n \mathcal{C}_{\mathbf{k}_1 \mathbf{k}_2 \dots \mathbf{k}_r}^{\alpha}. \quad (76)$$

Again we have appealed to replica permutation symmetry in order to reinstate the dependence on the zeroth-replica wave vectors. The distributions  $\mathcal{M}_r$  are natural generalizations of the distribution of local density fluctuations, explored, e.g., in Ref. 10.

## IX. CONCLUDING REMARKS

In this paper we have identified the long wavelength, low energy Goldstone-type fluctuations of the amorphous solid state, and investigated their physical consequences. By constructing an effective free energy governing these fluctuations, we have determined the elastic properties of the amorphous solid, including its static shear modulus which, we have reconfirmed, vanishes as the third power of the amount by which the constraint density exceeds its critical value (at the classical level). We have also analyzed the effect of these fluctuations on the amorphous solid order parameter, finding that, in spatial dimensions greater than two, they induce a simple, rigid shift of the distribution of (squared) localization lengths. In addition, we have explored the properties of the

order-parameter correlations in the amorphous solid state, establishing their physical content in terms of a joint probability distribution characterizing pairs of localized particles. Moreover, we have computed the corresponding correlator induced by Goldstone-type fluctuations and, hence, obtained a specific formula for this joint probability distribution.

We have paid particular attention to systems of spatial dimension two. In this setting we have shown that fluctuations restore the symmetries broken spontaneously at the classical level, particle localization is destroyed, the order parameter is driven to zero, and order-parameter correlations decay as a power law in the separation between points in the sample. The state is a *quasiamorphous solid* state, inasmuch as it possesses algebraically decaying correlations and rigidity.

Our work can be extended in several directions. We have focused here on the critical behavior of the shear modulus. It is also of interest to study elasticity in the strongly crosslinked limit, in which (geometrical and thermal) fluctuations are less important and mean-field theory should even be quantitatively correct. Whereas for long-chain macromolecules this limit is difficult to achieve, it may well be possible for Brownian particles, i.e., networks that are built from small units, in the simplest case just monomers.<sup>16</sup> Even more interesting is a generalization to nonlinear elasticity. Rubber can withstand very large deformations—up to 1000%—thus allowing large amounts of elastic energy to be stored in the system. Our approach can be generalized to include nonlinear terms in the strain tensor, which will arise from two sources: the expansion of the Goldstone-type fluctuations (11a) and higher-order nonlinearities in the Landau-Wilson free energy (23). Work along these lines is in progress.

#### ACKNOWLEDGMENTS

Certain ideas concerning the nature of the vulcanization transition in two spatial dimensions, developed in detail in the present paper, originated in enlightening discussions involving Horacio E. Castillo and Weiqun Peng; see Refs. 3 and 14. It is a pleasure to acknowledge these discussions, as well as enlightening discussions with Matthew P. A. Fisher, Dominique Toublan, and Michael Stone. The authors thank for their hospitality the Department of Physics at the University of Colorado–Boulder (P.M.G.) and the Kavli Institute for

Theoretical Physics at the University of California–Santa Barbara (P.M.G. and A.Z.), where some of the work reported here was undertaken. This work was supported in part by the National Science Foundation under Grants No. NSF DMR02-05858 (P.M.G. and S.M.), No. NSF PH99-07949 (P.M.G. and A.Z.), and by the DFG through SFB 602 and Grant No. Zi 209/6-1 (A.Z.).

#### APPENDIX A: FROM LANDAU-WILSON HAMILTONIAN TO ELASTIC FREE ENERGY

In this appendix we show how to get from the Landau-Wilson effective Hamiltonian  $\mathcal{S}_\Omega$ , Eq. (23), to the elastic free energy (27b). Specifically, we compute the increase  $\mathcal{S}_u$  in  $\mathcal{S}_\Omega$  when the classical value  $\Omega_{cl}$ , Eqs. (6) and (26), is replaced by Goldstone-distorted classical state (11a), parametrized by  $u_\tau(\mathbf{x})$ . There are three terms in (23) to be computed. Two are “potential,” terms, which we shall see to have no dependence on  $u_\tau(\mathbf{x})$ ; the third is a “gradient” term, and this is the origin of the dependence of  $\mathcal{S}_u$  on  $u_\tau(\mathbf{x})$ .

Before focusing on any individual terms, we note that we can express summations over higher-replica sector wave vectors as unrestricted summations, less lower-replica sector contributions; e.g.,

$$\sum_{k \in \text{HRS}} = \sum_k - \sum_{k \in \text{1RS}} - \sum_{k \in \text{0RS}}. \quad (\text{A1})$$

Here, the two components of the lower-replica sector, viz., the one- and zero-replica sectors, are, respectively, denoted 1RS and 0RS.

Applying this sector decomposition to the first term in Eq. (23), and recognizing that there is no contribution from the one-replica sector and that the zero-replica sector contribution is simple, we have

$$\begin{aligned} \sum_{k \in \text{HRS}} |\Omega(k)|^2 &= \left( \sum_k - \sum_{k \in \text{1RS}} - \sum_{k \in \text{0RS}} \right) |\Omega(k)|^2 \\ &= \sum_k |\Omega(k)|^2 - 0 - Q^2. \end{aligned} \quad (\text{A2})$$

Recall that we are concerned with the increase in  $\mathcal{S}_\Omega$  due to the Goldstone distortion. Evidently, of the contributions considered so far only the unrestricted sum has the possibility of being sensitive to the distortion. However, as we shall now see, not even this contribution has such sensitivity:

$$\begin{aligned} \frac{1}{V^n} \sum_k |\Omega(k)|^2 &= V \int dk_\lambda dk_\tau \int \frac{d\mathbf{x}_1}{V} \frac{d\mathbf{x}_2}{V} e^{-i\mathbf{k}_{\text{tot}} \cdot \mathbf{x}_1 + i\mathbf{k}_{\text{tot}} \cdot \mathbf{x}_2} e^{-ik_\tau u_\tau(\mathbf{x}_1) + ik_\tau u_\tau(\mathbf{x}_2)} \mathcal{W}(k_\tau)^2 \\ &= V \int \frac{d\mathbf{x}_1}{V} \frac{d\mathbf{x}_2}{V} \int dk_\tau \mathcal{W}(k_\tau)^2 e^{-ik_\tau (u_\tau(\mathbf{x}_1) - u_\tau(\mathbf{x}_2))} \int dk_\lambda e^{-i\mathbf{k}_{\text{tot}} \cdot (\mathbf{x}_1 - \mathbf{x}_2)} \\ &= V \int \frac{d\mathbf{x}_1}{V} \frac{d\mathbf{x}_2}{V} \int dk_\tau \mathcal{W}(k_\tau)^2 e^{-ik_\tau (u_\tau(\mathbf{x}_1) - u_\tau(\mathbf{x}_2))} (1+n)^{-D/2} \delta(\mathbf{x}_1 - \mathbf{x}_2) \\ &= (1+n)^{-D/2} \int dk_\tau \mathcal{W}(k_\tau)^2, \end{aligned} \quad (\text{A3})$$

independent of  $u_\tau(\mathbf{x})$ . Note that here and elsewhere in the present appendix we shall anticipate the taking of the replica limit by omitting factors of  $V^n$ .

Turning to the third term in (23), the nonlinearity, and handling the constraints on the summation with care, we are faced with the term

$$\begin{aligned}
V \sum_{k_1, k_2, k_3} \delta_{k_1+k_2+k_3, 0} \Omega(k_1) \Omega(k_2) \Omega(k_3) &= \int d\mathbf{k}_1 d\mathbf{k}_2 d\mathbf{k}_3 \int d\mathbf{y} e^{-i\mathbf{y} \cdot (k_1+k_2+k_3)} \\
&\times \int d\mathbf{x}_1 d\mathbf{x}_2 d\mathbf{x}_3 e^{i\mathbf{k}_1 \cdot \text{tot} \cdot \mathbf{x}_1 + i\mathbf{k}_2 \cdot \text{tot} \cdot \mathbf{x}_2 + i\mathbf{k}_3 \cdot \text{tot} \cdot \mathbf{x}_3} e^{ik_{1\tau} u_\tau(\mathbf{x}_1) + ik_{2\tau} u_\tau(\mathbf{x}_2) + ik_{3\tau} u_\tau(\mathbf{x}_3)} \mathcal{W}(k_{1\tau}) \mathcal{W}(k_{2\tau}) \mathcal{W}(k_{3\tau}) \\
&= \int d\mathbf{k}_{1\lambda} d\mathbf{k}_{2\lambda} d\mathbf{k}_{3\lambda} \int \frac{d\mathbf{y}_\lambda}{V} e^{-i\mathbf{y}_\lambda \cdot (k_{1\lambda} + k_{2\lambda} + k_{3\lambda})} \int d\mathbf{k}_{1\tau} d\mathbf{k}_{2\tau} d\mathbf{k}_{3\tau} \int d\mathbf{y}_\tau e^{-i\mathbf{y}_\tau \cdot (k_{1\tau} + k_{2\tau} + k_{3\tau})} \\
&\times \int d\mathbf{x}_1 d\mathbf{x}_2 d\mathbf{x}_3 e^{i\mathbf{k}_1 \cdot \text{tot} \cdot \mathbf{x}_1 + i\mathbf{k}_2 \cdot \text{tot} \cdot \mathbf{x}_2 + i\mathbf{k}_3 \cdot \text{tot} \cdot \mathbf{x}_3} e^{ik_{1\tau} u_\tau(\mathbf{x}_1) + ik_{2\tau} u_\tau(\mathbf{x}_2) + ik_{3\tau} u_\tau(\mathbf{x}_3)} \mathcal{W}(k_{1\tau}) \mathcal{W}(k_{2\tau}) \mathcal{W}(k_{3\tau}) \\
&= (1+n)^D \int d\mathbf{k}_1 d\mathbf{k}_2 d\mathbf{k}_3 \int \frac{d\mathbf{y}}{V} e^{-i\mathbf{y} \cdot (\mathbf{k}_1 + \mathbf{k}_2 + \mathbf{k}_3)} \int d\mathbf{k}_{1\tau} d\mathbf{k}_{2\tau} d\mathbf{k}_{3\tau} \int d\mathbf{y}_\tau e^{-i\mathbf{y}_\tau \cdot (k_{1\tau} + k_{2\tau} + k_{3\tau})} \\
&\times \int d\mathbf{x}_1 d\mathbf{x}_2 d\mathbf{x}_3 e^{i\mathbf{k}_1 \cdot \mathbf{x}_1 + i\mathbf{k}_2 \cdot \mathbf{x}_2 + i\mathbf{k}_3 \cdot \mathbf{x}_3} e^{ik_{1\tau} u_\tau(\mathbf{x}_1) + ik_{2\tau} u_\tau(\mathbf{x}_2) + ik_{3\tau} u_\tau(\mathbf{x}_3)} \mathcal{W}(k_{1\tau}) \mathcal{W}(k_{2\tau}) \mathcal{W}(k_{3\tau}) \\
&= (1+n)^D \int d\mathbf{k}_{1\tau} d\mathbf{k}_{2\tau} d\mathbf{k}_{3\tau} \delta_{k_{1\tau} + k_{2\tau} + k_{3\tau}, 0} \int \frac{d\mathbf{y}}{V} \int d\mathbf{x}_1 d\mathbf{x}_2 d\mathbf{x}_3 \delta(\mathbf{x}_1 - \mathbf{y}) \delta(\mathbf{x}_2 - \mathbf{y}) \delta(\mathbf{x}_3 - \mathbf{y}) \\
&\times e^{ik_{1\tau} u_\tau(\mathbf{x}_1) + ik_{2\tau} u_\tau(\mathbf{x}_2) + ik_{3\tau} u_\tau(\mathbf{x}_3)} \mathcal{W}(k_{1\tau}) \mathcal{W}(k_{2\tau}) \mathcal{W}(k_{3\tau}) \\
&= (1+n)^D \int d\mathbf{k}_{1\tau} d\mathbf{k}_{2\tau} d\mathbf{k}_{3\tau} \delta_{k_{1\tau} + k_{2\tau} + k_{3\tau}, 0} \int \frac{d\mathbf{y}}{V} e^{i(k_{1\tau} + k_{2\tau} + k_{3\tau}) \cdot u_\tau(\mathbf{y})} \mathcal{W}(k_{1\tau}) \mathcal{W}(k_{2\tau}) \mathcal{W}(k_{3\tau}) \\
&= (1+n)^D \int d\mathbf{k}_{1\tau} d\mathbf{k}_{2\tau} d\mathbf{k}_{3\tau} \delta_{k_{1\tau} + k_{2\tau} + k_{3\tau}, 0} \mathcal{W}(k_{1\tau}) \mathcal{W}(k_{2\tau}) \mathcal{W}(k_{3\tau}). \tag{A4}
\end{aligned}$$

This is independent of  $u_\tau(\mathbf{x})$ .

Turning to the second term in (23), the gradient term, we have

$$\frac{1}{V^n} \sum_k k \cdot k |\Omega(k)|^2 = V \int d\mathbf{k}_\lambda d\mathbf{k}_\tau (k_\lambda \cdot k_\lambda + k_\tau \cdot k_\tau) \int \frac{d\mathbf{x}_1 d\mathbf{x}_2}{V} e^{-i\mathbf{k}_{\text{tot}} \cdot \mathbf{x}_1 + i\mathbf{k}_{\text{tot}} \cdot \mathbf{x}_2} \times e^{-ik_\tau u_\tau(\mathbf{x}_1) + ik_\tau u_\tau(\mathbf{x}_2)} \mathcal{W}(k_\tau)^2. \tag{A5}$$

Of the two contributions arising from this term, from  $k_\lambda^2$  and from  $k_\tau^2$ , the latter has no  $u_\tau(\mathbf{x})$  dependence. This follows via the mechanism that we saw for the first term, viz., the development of a factor of  $\delta(\mathbf{x}_1 - \mathbf{x}_2)$ . As for the former contribution, to evaluate it we replace  $k_\lambda \cdot k_\lambda$  by  $(1+n)^{-1} \mathbf{k}_{\text{tot}} \cdot \mathbf{k}_{\text{tot}}$  and generate this factor via suitable derivatives,

$$\begin{aligned}
\frac{1}{V^n} \sum_k k \cdot k |\Omega(k)|^2 &= V \int d\mathbf{k}_\lambda d\mathbf{k}_\tau k_\lambda \cdot k_\lambda \int \frac{d\mathbf{x}_1 d\mathbf{x}_2}{V} e^{-i\mathbf{k}_{\text{tot}} \cdot \mathbf{x}_1 + i\mathbf{k}_{\text{tot}} \cdot \mathbf{x}_2} e^{-ik_\tau u_\tau(\mathbf{x}_1) + ik_\tau u_\tau(\mathbf{x}_2)} \mathcal{W}(k_\tau)^2 \\
&= (1+n)^{-D/2} (1+n)^{-1} V \int d\mathbf{k}_\tau d\mathbf{k}_{\text{tot}} \int \frac{d\mathbf{x}_1 d\mathbf{x}_2}{V} (\partial_{-i\mathbf{x}_1} e^{-i\mathbf{k}_{\text{tot}} \cdot \mathbf{x}_1}) \cdot (\partial_{i\mathbf{x}_2} e^{i\mathbf{k}_{\text{tot}} \cdot \mathbf{x}_2}) e^{-ik_\tau u_\tau(\mathbf{x}_1)} e^{ik_\tau u_\tau(\mathbf{x}_2)} \mathcal{W}(k_\tau)^2. \tag{A6}
\end{aligned}$$

Next, we integrate by parts, once with respect to  $\mathbf{x}_1$  and once with respect to  $\mathbf{x}_2$ , to transfer the derivatives to the exponential factors containing  $u_\tau$ , arriving at

$$(1+n)^{-1-D/2} V \int \frac{d\mathbf{x}_1 d\mathbf{x}_2}{V} \times \int d\mathbf{k}_{\text{tot}} e^{-i\mathbf{k}_{\text{tot}} \cdot (\mathbf{x}_1 - \mathbf{x}_2)} \int dk_\tau \mathcal{W}(k_\tau)^2 \times (\partial_{-ix_1} e^{-ik_\tau u_\tau(\mathbf{x}_1)}) \cdot (\partial_{ix_2} e^{ik_\tau u_\tau(\mathbf{x}_2)}). \quad (\text{A7})$$

Powers of  $k_\lambda$  higher than two would, via the corresponding derivatives, produce higher gradients of  $u_\tau$ , as well as nonlinearities involving lower-order derivatives. By performing the derivatives that we have here, as well as the  $\mathbf{k}_{\text{tot}}$  integration, which generates a factor  $\delta(\mathbf{x}_1 - \mathbf{x}_2)$  and allows us to integrate over, say,  $\mathbf{x}_2$ , we obtain

$$(1+n)^{-1-D/2} V^{-1} \int dk_\tau \mathcal{W}(k_\tau)^2 \times \int d\mathbf{x} (k_\tau \cdot \partial_{\mathbf{x}} u_\tau(\mathbf{x})) \cdot (k_\tau \cdot \partial_{\mathbf{x}} u_\tau(\mathbf{x})), \quad (\text{A8})$$

where the scalar products inside the parentheses are over  $nD$ -component replica-transverse vectors while the outside scalar product is over  $D$ -component position vectors. The next step is to observe that, owing to the rotationally invariant form of  $\mathcal{W}(k_\tau)$ , Eq. (26a), the  $k_\tau$  integration includes an isotropic average of two components of  $k_\tau$ , and is therefore proportional to the identity in  $nD$ -dimensional replica-transverse space. Thus, we arrive at the form

$$\frac{(1+n)^{-1-D/2}}{nD} \int dk_\tau \mathcal{W}(k_\tau)^2 k_\tau \cdot k_\tau \int \frac{d\mathbf{x}}{V} (\partial_{\mathbf{x}} u_\tau(\mathbf{x})) \partial_{\mathbf{x}} u_\tau(\mathbf{x}), \quad (\text{A9})$$

which involves the two types of scalar product mentioned beneath Eq. (A8). Reinstating the factor of  $Vc$  from Eq. (23), we identify the stiffness divided by the temperature  $\mu_n/T$  and, hence, arrive at Eqs. (27).

#### APPENDIX B: EVALUATING THE STIFFNESS (ALSO KNOWN AS SHEAR MODULUS OR RIGIDITY)

In this appendix we display the main steps for obtaining the stiffness  $\mu_0$ , Eqs. (28), by evaluating the formula for  $\mu_n$ , given in Eq. (27b) and derived in Appendix A, in terms of the elements of the classical state, Eqs. (26). This involves the evaluation of the right-hand side (RHS) of Eq. (27b), which proceeds as follows:

$$\begin{aligned} \int dk_\tau k_\tau^2 \mathcal{W}(k_\tau)^2 &= Q^2 \int dk_\tau k_\tau^2 \int_0^\infty d\xi^2 \mathcal{N}(\xi^2) d\xi'^2 \mathcal{N}(\xi'^2) e^{-(\xi^2 + \xi'^2) k_\tau^2 / 2} \\ &= Q^2 \int_0^\infty d\xi^2 \mathcal{N}(\xi^2) d\xi'^2 \mathcal{N}(\xi'^2) \int dk_\tau k_\tau^2 e^{-(\xi^2 + \xi'^2) k_\tau^2 / 2} \\ &= Q^2 \int_0^\infty d\xi^2 \mathcal{N}(\xi^2) d\xi'^2 \mathcal{N}(\xi'^2) \partial_{-A/2} |_{A=\xi^2 + \xi'^2} \int dk_\tau e^{-A k_\tau^2 / 2} \\ &= Q^2 \int_0^\infty d\xi^2 \mathcal{N}(\xi^2) d\xi'^2 \mathcal{N}(\xi'^2) \partial_{-A/2} |_{A=\xi^2 + \xi'^2} (2\pi A)^{-nD/2} \\ &= Q^2 \int_0^\infty d\xi^2 \mathcal{N}(\xi^2) d\xi'^2 \mathcal{N}(\xi'^2) nD (2\pi A)^{-nD/2} A^{-1} |_{A=\xi^2 + \xi'^2} \\ &\stackrel{n \rightarrow 0}{\approx} nD Q^2 \int_0^\infty d\xi^2 \mathcal{N}(\xi^2) d\xi'^2 \mathcal{N}(\xi'^2) (\xi^2 + \xi'^2)^{-1}. \end{aligned} \quad (\text{B1})$$

#### APPENDIX C: ELASTIC GREEN FUNCTION

The elastic Green function  $\mathcal{G}_{dd'}(\mathbf{x} - \mathbf{x}')$  featuring in Eq. (31a) arises via functional integration over the displacement field  $\mathbf{u}(\mathbf{x})$ . This integration comprises fields configurations that are (i) volume preserving (at least to leading order in the gradient of the displacement field) and (ii) have Fourier content only from wavelengths lying between the short- and long-distance cutoffs



$\ell_<$  and  $\ell_>$ . As the weight in Eq. (31a) is Gaussian with respect to  $\mathbf{u}(\mathbf{x})$ , we have that  $(T/\mu_0)\mathcal{G}_{dd'}(\mathbf{x}-\mathbf{x}')$  is proportional to the inverse of the operator appearing sandwiched between two displacement fields in the exponent of the Gaussian,

$$\frac{\mu_0}{T} \int_{\mathcal{V}} d\mathbf{x} (\partial_{\mathbf{x}} \mathbf{u} \cdot \partial_{\mathbf{x}} \mathbf{u}), \quad (\text{C1})$$

provided this inverse is the one associated with the Hilbert space of vector-field configurations contributing to the functional integral. An application of the divergence theorem shows that, in addition to conditions (i) and (ii), the Green function obeys the equation

$$-\nabla_{\mathbf{x}}^2 \mathcal{G}_{dd'}(\mathbf{x}) = \delta_{dd'} \delta(\mathbf{x}), \quad (\text{C2})$$

in which the delta function is to be interpreted as the identity in the appropriate Hilbert space, mentioned above. To determine  $\mathcal{G}_{dd'}(\mathbf{x})$  we express it in its Fourier representation,

$$\mathcal{G}_{dd'}(\mathbf{x}) = \int d\mathbf{k} e^{-i\mathbf{k}\cdot\mathbf{x}} \mathcal{G}_{dd'}(\mathbf{k}). \quad (\text{C3})$$

Next, we insert this representation into Eq. (C2) to obtain

$$-\nabla_{\mathbf{x}}^2 \int d\mathbf{k} e^{-i\mathbf{k}\cdot\mathbf{x}} \mathcal{G}_{dd'}(\mathbf{k}) = \int d\mathbf{k} k^2 e^{-i\mathbf{k}\cdot\mathbf{x}} \mathcal{G}_{dd'}(\mathbf{k}) = \int_{2\pi/\ell_>}^{2\pi/\ell_<} d\mathbf{k} e^{-i\mathbf{k}\cdot\mathbf{x}} (\delta_{dd'} - k^{-2} k_d k_{d'}), \quad (\text{C4})$$

where  $\ell_< \equiv \ell_</2\pi$  and  $\ell_> \equiv \ell_>/2\pi$ . The final term, the integral representation of the appropriate delta function, accommodates restrictions (i) and (ii). Then, from the linear independence of the plane waves, we see that the Fourier integral representation of the Green function is given by Eq. (C3), with the amplitude given by

$$\mathcal{G}_{dd'}(\mathbf{k}) = \begin{cases} (k^2 \delta_{dd'} - k_d k_{d'})/k^4 & \text{for } \ell_>^{-1} < k < \ell_<^{-1}, \\ 0 & \text{otherwise,} \end{cases} \quad (\text{C5})$$

as given in Eq. (31b).

Before computing the real-space form of this  $D$ -dimensional Green function, we evaluate it at argument  $\mathbf{x}=\mathbf{0}$ , as well as at small argument ( $|\mathbf{x}| \ll \ell_<$ ). At  $\mathbf{x}=\mathbf{0}$  we have

$$\mathcal{G}_{dd'}(\mathbf{x})|_{\mathbf{x}=\mathbf{0}} = \int_{\text{hco}} d\mathbf{k} (k^2 \delta_{dd'} - k_d k_{d'}) k^{-4} \quad (\text{C6a})$$

$$= \delta_{dd'} \frac{D-1}{D} \int_{\text{hco}} d\mathbf{k} k^{-2} \quad (\text{C6b})$$

$$= \delta_{dd'} \Gamma_D, \quad (\text{C6c})$$

$$\Gamma_D \equiv \frac{D-1}{D} \frac{\Sigma_D}{(2\pi)^D} \int_{\ell_>^{-1}}^{\ell_<^{-1}} dk k^{D-3}. \quad (\text{C6d})$$

Here and elsewhere, the subscript hco indicates that the integration is subject to the hard cutoff shown explicitly in Eq. (C6d). Evaluating the last integral for  $D \geq 2$ , and for  $D > 2$  retaining only the dominant contribution, gives  $\Gamma_D$ , as given in Eq. (37).

Now generalizing to  $|\mathbf{x}|$  small but nonzero, i.e.,  $|\mathbf{x}| \ll \ell_<$ , we have, by expanding the exponential in Eq. (C3),

$$\mathcal{G}_{dd'}(\mathbf{x}) \approx \delta_{dd'} \Gamma_D - \frac{1}{2} [(D+1)\delta_{dd'} - 2\hat{x}_d \hat{x}_{d'}] |\mathbf{x}|^2 \times \frac{\Sigma_D}{(2\pi)^D} \frac{1}{D(D+2)} \int_{\ell_>^{-1}}^{\ell_<^{-1}} dk k^{D-1} \quad (\text{C7})$$

$$\begin{aligned} &\approx \delta_{dd'} \Gamma_D - \frac{1}{2} [(D+1) \delta_{dd'} - 2 \hat{x}_d \hat{x}_{d'}] |\mathbf{x}|^2 \\ &\times \frac{\sum_D}{\ell_{<}^D} \frac{1}{D^2(D+2)}, \end{aligned} \tag{C8}$$

where, again, we have retained only the dominant contribution. Specializing to  $D=2$  and  $D=3$  we find

$$\mathcal{G}_{dd'}^{(2)}(\mathbf{x}) \approx \delta_{dd'} \Gamma_2 - \frac{1}{64\pi} \frac{|\mathbf{x}|^2}{\ell_{<}^2} (3 \delta_{dd'} - 2 \hat{x}_d \hat{x}_{d'}), \tag{C9}$$

$$\mathcal{G}_{dd'}^{(3)}(\mathbf{x}) \approx \delta_{dd'} \Gamma_3 - \frac{1}{45\pi \ell_{<}} \frac{|\mathbf{x}|^2}{\ell_{<}^2} (2 \delta_{dd'} - \hat{x}_d \hat{x}_{d'}). \tag{C10}$$

We now compute the real-space form of this  $D$ -dimensional Green function, valid for arbitrary  $|\mathbf{x}|$ ,

$$\mathcal{G}_{dd'}(\mathbf{x}) = \int d\mathbf{k} e^{-i\mathbf{k}\cdot\mathbf{x}} \mathcal{G}_{dd'}(\mathbf{k}) \tag{C11}$$

$$= \int_{\text{hco}} d\mathbf{k} e^{-i\mathbf{k}\cdot\mathbf{x}} (k^2 \delta_{dd'} - k_d k_{d'}) k^{-4} \tag{C12}$$

$$= -(\delta_{dd'} \nabla^2 - \partial_d \partial_{d'}) \mathcal{H}(\mathbf{x}), \tag{C13}$$

$$\mathcal{H}(\mathbf{x}) \equiv \int_{\text{hco}} d\mathbf{k} e^{-i\mathbf{k}\cdot\mathbf{x}} k^{-4} \tag{C14}$$

$$= \int_{\ell_{>}^{-1}}^{\ell_{<}^{-1}} dk k^{D-1} \int d^{D-1} \hat{\mathbf{k}} \frac{e^{-i\mathbf{k}\cdot\mathbf{x}}}{k^4}. \tag{C15}$$

Specializing to the case of  $D=3$ , and using spherical polar coordinates  $(k, \theta, \varphi)$ , we have

$$\mathcal{H}^{(3)}(\mathbf{x}) = (2\pi)^{-3} \int_{\ell_{>}}^{\ell_{<}} \frac{dk}{k^2} \int_0^{2\pi} d\varphi \int_0^\pi d\theta \sin \theta e^{-ik|\mathbf{x}|\cos \theta} = \frac{|\mathbf{x}|/\ell_{<}}{2\pi^2} \int_{|\mathbf{x}|/\ell_{>}}^{|\mathbf{x}|/\ell_{<}} dz \frac{\sin z}{z^3}. \tag{C16}$$

To control the potential divergence at small  $z$  we add and subtract the small- $z$  behavior of  $\sin z$ , thus obtaining

$$\mathcal{H}^{(3)}(\mathbf{x}) = \frac{|\mathbf{x}|}{2\pi^2} \int_{|\mathbf{x}|/\ell_{>}}^{|\mathbf{x}|/\ell_{<}} dz \left( \frac{\sin z - z}{z^3} + \frac{1}{z^2} \right) \tag{C17}$$

$$= \frac{|\mathbf{x}|}{2\pi^2} (\text{Si}_3(|\mathbf{x}|/\ell_{<}) - \text{Si}_3(|\mathbf{x}|/\ell_{>})) + \frac{\ell_{>} - \ell_{<}}{2\pi^2}, \tag{C18}$$

$$\text{Si}_3(t) \equiv \int_0^t dz \frac{\sin z - z}{z^3}, \tag{C19}$$

where  $\text{Si}_3(z)$  is a generalized sine integral, which has asymptotic behavior

$$\text{Si}_3(t) \approx \begin{cases} -t/3! & \text{for } t \ll 1, \\ -(\pi/4) - t^{-1} & \text{for } t \gg 1. \end{cases} \tag{C20}$$

Using this behavior to approximate  $\mathcal{H}^{(3)}(\mathbf{x})$  in Eq. (C18), and inserting the result into Eq. (C13), noting that the final term vanishes under differentiation, we obtain for  $\ell_{<} \ll |\mathbf{x}| \ll \ell_{>}$ ,

$$\mathcal{G}_{dd'}^{(3)}(\mathbf{x}) \approx (\delta_{dd'} \nabla^2 - \partial_d \partial_{d'}) \frac{|\mathbf{x}|}{8\pi} \quad (\text{C21})$$

$$= \frac{1}{8\pi|\mathbf{x}|} (\delta_{dd'} + \hat{x}_d \hat{x}_{d'}). \quad (\text{C22})$$

Now specializing to the case of  $D=2$ , and using plane polar coordinates  $(k, \varphi)$ , we have

$$\mathcal{H}^{(2)}(\mathbf{x}) = (2\pi)^{-2} \int_{\ell_{>}^{-1}}^{\ell_{<}^{-1}} \frac{dk}{k} \int_0^{2\pi} d\varphi e^{-ik|\mathbf{x}|\cos\varphi} = \frac{|\mathbf{x}|^2}{2\pi} \int_{|\mathbf{x}|/\ell_{>}}^{|\mathbf{x}|/\ell_{<}} \frac{dz}{z^3} \int_0^{2\pi} d\varphi e^{-iz\cos\varphi}. \quad (\text{C23})$$

To control the potential divergence at small  $z$  we add and subtract the small- $z$  behavior of the integrand, thus obtaining

$$\mathcal{H}^{(2)}(\mathbf{x}) = \frac{|\mathbf{x}|^2}{2\pi} \int_{|\mathbf{x}|/\ell_{>}}^{|\mathbf{x}|/\ell_{<}} \frac{dz}{z^3} \int_0^{2\pi} d\varphi (e^{-iz\cos\varphi} - (1 - \frac{1}{4}z^2)) + \frac{|\mathbf{x}|^2}{2\pi} \int_{|\mathbf{x}|/\ell_{>}}^{|\mathbf{x}|/\ell_{<}} \frac{dz}{z^3} (1 - \frac{1}{4}z^2) \quad (\text{C24})$$

$$= \frac{|\mathbf{x}|^2}{2\pi} (\mathcal{S}(|\mathbf{x}|/\ell_{<}) - \mathcal{S}(|\mathbf{x}|/\ell_{>})) + \frac{\ell_{>}^2 - \ell_{<}^2}{4\pi} - \frac{|\mathbf{x}|^2}{8\pi} \ln(\ell_{>}/\ell_{<}), \quad (\text{C25})$$

$$\mathcal{S}(t) \equiv \int_0^t \frac{dz}{z^3} \int_0^{2\pi} d\varphi (e^{-iz\cos\varphi} - (1 - \frac{1}{4}z^2)). \quad (\text{C26})$$

Noting that  $\mathcal{S}(t)$  has asymptotic behavior<sup>17</sup>

$$\mathcal{S}(t) \approx \begin{cases} \frac{1}{128}t^2 & \text{for } t \ll 1, \\ \frac{1}{4} \ln(t/2e^{1-\gamma}) & \text{for } t \gg 1, \end{cases} \quad (\text{C27})$$

where  $\gamma(=0.5772\cdots)$  is the Euler-Mascheroni constant and using this to approximate  $\mathcal{H}^{(2)}(\mathbf{x})$  in Eq. (C25), and inserting the result into Eq. (C13), noting that the constant term vanishes under differentiation, we obtain for  $\ell_{<} \ll |\mathbf{x}| \ll \ell_{>}$  the result

$$\mathcal{G}_{dd'}^{(2)}(\mathbf{x}) \approx -\frac{1}{4\pi} (\delta_{dd'} \ln(e^{\gamma+1/2} |\mathbf{x}|/2\ell_{>}) - \hat{x}_d \hat{x}_{d'}). \quad (\text{C28})$$

#### APPENDIX D: FROM THE CORRELATOR TO THE DISTRIBUTION

In this appendix we give the technical steps involved in going from the two-field correlator to the distribution  $\mathcal{P}$ , as discussed in Sec. VIII B. Beginning with Eq. (69), setting  $\mathbf{k}_{2 \text{ tot}}$  to be  $\mathbf{k}_{1 \text{ tot}}$ , and reorganizing, we obtain

$$\begin{aligned} & Q^2 \int d\Delta r_{11} d\Delta r_{22} d\Delta r_{12} e^{-1/2\Delta r_{11d_1d_2} \sum_{\alpha=0}^n k_{1d_1}^{\alpha} k_{1d_2}^{\alpha} - 1/2\Delta r_{22d_1d_2} \sum_{\alpha=0}^n k_{2d_1}^{\alpha} k_{2d_2}^{\alpha} + \Delta r_{12d_1d_2} \sum_{\alpha=0}^n k_{1d_1}^{\alpha} k_{2d_2}^{\alpha}} \\ & \times \int d\mathbf{x} e^{i\mathbf{k}_{\text{tot}} \cdot \mathbf{x}} \mathcal{P}(\mathbf{x}, \Delta r_{11}, \Delta r_{22}, \Delta r_{12}) = \overline{\mathcal{W}}(k_{1\tau}) \overline{\mathcal{W}}(k_{2\tau}) \int \frac{d\mathbf{x}}{V} e^{i\mathbf{k}_{1 \text{ tot}} \cdot \mathbf{x}} e^{(T/\mu_0) \mathcal{G}_{d_1 d_2}(\mathbf{x}) k_{1\tau d_1} \cdot k_{2\tau d_2}}. \end{aligned} \quad (\text{D1})$$

Inserting the parametrization (70) for  $\mathcal{P}$ , performing the resulting integrations over  $\Delta r_{11}$ ,  $\Delta r_{22}$ , and  $\Delta r_{12}$  on the left-hand side (LHS), exchanging factors of  $\overline{\mathcal{W}}$  for  $\tilde{\mathcal{N}}$  via Eq. (36b), canceling factors of  $Q$ , and identifying the Fourier transform

$$\mathcal{P}(\mathbf{q}, \xi_1^2, \xi_2^2, \mathbf{y}) \equiv \int d\mathbf{x} e^{i\mathbf{q} \cdot \mathbf{x}} \mathcal{P}(\mathbf{x}, \xi_1^2, \xi_2^2, \mathbf{y}), \quad (\text{D2})$$

we arrive at the following equation:

$$\begin{aligned}
& \int d\xi_1^2 \tilde{\mathcal{N}}(\xi_1^2) d\xi_2^2 \tilde{\mathcal{N}}(\xi_2^2) d\mathbf{y} \mathcal{P}(\mathbf{k}_{1 \text{ tot}}, \xi_1^2, \xi_2^2, \mathbf{y}) e^{-1/2\xi_1^2 k_{1\tau}^2 - 1/2\xi_2^2 k_{2\tau}^2 + (T/\mu_0)\mathcal{G}_{d_1 d_2}(\mathbf{y}) k_{1 d_1} \cdot k_{2 d_2}} \\
& = \int d\xi_1^2 \tilde{\mathcal{N}}(\xi_1^2) d\xi_2^2 \tilde{\mathcal{N}}(\xi_2^2) e^{-1/2\xi_1^2 k_{1\tau}^2 - 1/2\xi_2^2 k_{2\tau}^2} \int d\mathbf{y} e^{i\mathbf{k}_{1 \text{ tot}} \cdot \mathbf{x}} e^{(T/\mu_0)\mathcal{G}_{d_1 d_2}(\mathbf{y}) k_{1 \tau d_1} \cdot k_{2 \tau d_2}}. \tag{D3}
\end{aligned}$$

In order to clarify the content of this equation, we rewrite the wave-vector dependence on the LHS in terms of replica-longitudinal (more precisely,  $k_\tau$ ) and replica-transverse (in fact  $\mathbf{k}_{\text{tot}}$ ) components [see Eqs. (9) and (10b)], noting that  $\mathbf{k}_{1 \text{ tot}} = \mathbf{k}_{2 \text{ tot}}$  and writing  $\mathbf{q}$  for each, to obtain

$$\begin{aligned}
& \int d\xi_1^2 \tilde{\mathcal{N}}(\xi_1^2) d\xi_2^2 \tilde{\mathcal{N}}(\xi_2^2) \int d\mathbf{y} \mathcal{P}(\mathbf{q}, \xi_1^2, \xi_2^2, \mathbf{y}) e^{-1/2\xi_1^2 k_{1\tau}^2 - 1/2\xi_2^2 k_{2\tau}^2 + (T/\mu_0)\mathcal{G}_{d_1 d_2}(\mathbf{y}) k_{1 \tau d_1} \cdot k_{2 \tau d_2}} e^{-[\mathbf{q} \cdot \mathbf{q}/2(1+n)](\xi_1^2 + \xi_2^2) + (T/\mu_0)\mathcal{G}_{d_1 d_2}(\mathbf{y}) q_{d_1} q_{d_2}} \\
& = \int d\xi_1^2 \tilde{\mathcal{N}}(\xi_1^2) d\xi_2^2 \tilde{\mathcal{N}}(\xi_2^2) e^{-1/2\xi_1^2 k_{1\tau}^2 - 1/2\xi_2^2 k_{2\tau}^2} \int d\mathbf{y} e^{i\mathbf{q} \cdot \mathbf{y}} e^{(T/\mu_0)\mathcal{G}_{d_1 d_2}(\mathbf{y}) k_{1 \tau d_1} \cdot k_{2 \tau d_2}}. \tag{D4}
\end{aligned}$$

Next, we identify Laplace transformations with respect to  $\xi_1^2$  and  $\xi_2^2$ , equate the entities being transformed on the LHS and RHS, and take the replica limit, thus arriving at

$$\begin{aligned}
& e^{-1/2(\xi_1^2 + \xi_2^2)q^2} \int d\mathbf{y} \mathcal{P}(\mathbf{q}, \xi_1^2, \xi_2^2, \mathbf{y}) e^{(T/\mu_0)\mathcal{G}_{d_1 d_2}(\mathbf{y}) k_{1 \tau d_1} \cdot k_{2 \tau d_2}} e^{(T/\mu_0)\mathcal{G}_{d_1 d_2}(\mathbf{y}) q_{d_1} q_{d_2}} \\
& = \int d\mathbf{y} e^{i\mathbf{q} \cdot \mathbf{y}} e^{(T/\mu_0)\mathcal{G}_{d_1 d_2}(\mathbf{y}) k_{1 \tau d_1} \cdot k_{2 \tau d_2}}. \tag{D5}
\end{aligned}$$

The next steps are to move the Gaussian prefactor to the RHS, and to introduce the dummy variable  $\mathbf{g}$ , which takes on the values held by the second-rank tensor  $\mathcal{G}(\mathbf{y})$ ,

$$\begin{aligned}
& \int d\mathbf{g} e^{(T/\mu_0)\mathbf{g}_{d_1 d_2} k_{1 \tau d_1} \cdot k_{2 \tau d_2}} \int d\mathbf{y} \delta(\mathbf{g} - \mathcal{G}(\mathbf{y})) \mathcal{P}(\mathbf{q}, \xi_1^2, \xi_2^2, \mathbf{y}) e^{(T/\mu_0)\mathcal{G}_{d_1 d_2}(\mathbf{y}) q_{d_1} q_{d_2}} \\
& = \int d\mathbf{g} e^{(T/\mu_0)\mathbf{g}_{d_1 d_2} k_{1 \tau d_1} \cdot k_{2 \tau d_2}} e^{1/2(\xi_1^2 + \xi_2^2)q^2} \int d\mathbf{y} e^{i\mathbf{q} \cdot \mathbf{y}} \delta(\mathbf{g} - \mathcal{G}(\mathbf{y})). \tag{D6}
\end{aligned}$$

Again equating entities being transformed, this time being transformed with respect to  $\mathbf{g}$ , we find

$$\begin{aligned}
& \int d\mathbf{y} \delta(\mathbf{g} - \mathcal{G}(\mathbf{y})) \mathcal{P}(\mathbf{q}, \xi_1^2, \xi_2^2, \mathbf{y}) \\
& = e^{1/2(\xi_1^2 + \xi_2^2)q^2} \int d\mathbf{y} e^{i\mathbf{q} \cdot \mathbf{y}} \delta(\mathbf{g} - \mathcal{G}(\mathbf{y})) e^{-(T/\mu_0)\mathcal{G}_{d_1 d_2}(\mathbf{y}) q_{d_1} q_{d_2}}. \tag{D7}
\end{aligned}$$

Next, we equate entities being transformed as  $\int d\mathbf{y} \delta(\mathbf{g} - \mathcal{G}(\mathbf{y})) \cdots$ , thus arriving at the Fourier transform of the reduced distribution,

$$\mathcal{P}(\mathbf{q}, \xi_1^2, \xi_2^2, \mathbf{y}) = e^{1/2(\xi_1^2 + \xi_2^2)q^2} e^{i\mathbf{q} \cdot \mathbf{y}} e^{-(T/\mu_0)\mathcal{G}_{d_1 d_2}(\mathbf{y}) q_{d_1} q_{d_2}}. \tag{D8}$$

Finally, we invert the Fourier transform to arrive at the reduced distribution,

$$\mathcal{P}(\mathbf{x}, \xi_1^2, \xi_2^2, \mathbf{y}) = \int d\mathbf{q} e^{-i\mathbf{q} \cdot \mathbf{x}} \mathcal{P}(\mathbf{q}, \xi_1^2, \xi_2^2, \mathbf{y}) = \int d\mathbf{q} e^{-i\mathbf{q} \cdot (\mathbf{x} - \mathbf{y})} e^{1/2(\xi_1^2 + \xi_2^2)q^2} e^{-(T/\mu_0)\mathcal{G}_{d_1 d_2}(\mathbf{y}) q_{d_1} q_{d_2}}. \tag{D9}$$

Convergence of this inversion is furnished by the cutoff nature of the  $\mathbf{q}$  integration. Inserting this formula into the parametrization (70) we arrive at a formula for the full distribution,

$$\begin{aligned}
\mathcal{P}(\mathbf{x}, \Delta r_{11}, \Delta r_{22}, \Delta r_{12}) & = \int d\xi_1^2 \tilde{\mathcal{N}}(\xi_1^2) d\xi_2^2 \tilde{\mathcal{N}}(\xi_2^2) \delta(\Delta r_{11} - \xi_1^2) \delta(\Delta r_{22} - \xi_2^2) \\
& \quad \times \int \frac{d\mathbf{y}}{V} \left\{ \int d\mathbf{q} e^{-i\mathbf{q} \cdot (\mathbf{x} - \mathbf{y})} e^{1/2(\xi_1^2 + \xi_2^2)q^2} e^{-(T/\mu_0)\mathcal{G}_{d_1 d_2}(\mathbf{y}) q_{d_1} q_{d_2}} \right\} \delta[\Delta r_{12} - (T/\mu_0)\mathcal{G}(\mathbf{y})]. \tag{D10}
\end{aligned}$$

- <sup>1</sup>S. Mukhopadhyay, P. M. Goldbart, and A. Zippelius, *Europhys. Lett.* **67**, 49 (2004).
- <sup>2</sup>P. M. Goldbart, H. E. Castillo, and A. Zippelius, *Adv. Phys.* **45**, 393 (1996).
- <sup>3</sup>See, e.g., P. M. Goldbart, *J. Phys.: Condens. Matter* **12**, 6585 (2000).
- <sup>4</sup>H. E. Castillo, P. M. Goldbart, and A. Zippelius, *Europhys. Lett.* **28**, 519 (1994).
- <sup>5</sup>D. J. Wallace, "Perturbative approach to surface fluctuations," in *Recent Advances in Field Theory and Statistical Mechanics*, edited by J.-B. Zuber and R. Stora (Les Houches Session XXXIX, 1982) (North-Holland, Amsterdam, 1984), pp. 173–216.
- <sup>6</sup>H. E. Castillo, P. M. Goldbart, and A. Zippelius, *Phys. Rev. B* **60**, 14 702 (1999).
- <sup>7</sup>L. D. Landau and E. M. Lifshitz, *Theory of Elasticity* (Pergamon, Oxford, 1986).
- <sup>8</sup>H. Kleinert, *Gauge Fields in Solids* (World Scientific, Singapore, 1989), Vol. 2, p. 746.
- <sup>9</sup>R. T. Deam and S. F. Edwards, *Proc. R. Soc. London, Ser. A* **280**, 317 (1976).
- <sup>10</sup>W. Peng, H. E. Castillo, P. M. Goldbart, and A. Zippelius, *Phys. Rev. B* **57**, 839 (1998).
- <sup>11</sup>H. E. Castillo and P. M. Goldbart, *Phys. Rev. E* **58**, R24 (1998); **62**, 8159 (2000).
- <sup>12</sup>B. Jancovici, *Phys. Rev. Lett.* **19**, 20 (1967); H. J. Mikeska and H. Schmidt, *J. Low Temp. Phys.* **2**, 371 (1970).
- <sup>13</sup>D. R. Nelson, *Defects and Geometry in Condensed Matter Physics* (Cambridge University Press, Cambridge, UK, 2001).
- <sup>14</sup>W. Peng and P. M. Goldbart, *Phys. Rev. E* **61**, 3339 (2000).
- <sup>15</sup>H.-K. Janssen and O. Stenull, *Phys. Rev. E* **64**, 026119 (2001); W. Peng, P. M. Goldbart, and A. J. McKane, *ibid.* **64**, 031105 (2001).
- <sup>16</sup>K. Broderix, M. Weigt, and A. Zippelius, *Eur. Phys. J. A* **29**, 441 (2002).
- <sup>17</sup>We thank Michael Stone for guidance on this point.